Quaternary Science Reviews 79 (2013) 191–206

Contents lists available at SciVerse ScienceDirect

Quaternary Science Reviews

journal homepage: www.elsevier.com/locate/quascirev

Modelling past sea ice changes

H. Goosse [a,*], D.M. Roche [b,c], A. Mairesse [a], M. Berger [d]

[a] Université catholique de Louvain, Earth and Life Institute, Georges Lemaître Centre for Earth and Climate Research, Place Pasteur 3, B-1348 Louvain-la-Neuve, Belgium
[b] Laboratoire des Sciences du Climat et de l'Environnement (IPSL-CEA/INSU-CNRS/UVSQ), Gif-sur-Yvette, France
[c] Cluster Earth & Climate, Faculty of Earth and Life Sciences, Vrije Universiteit Amsterdam, Amsterdam, The Netherlands
[d] Royal Institute of Technology, KTH Department of Mechanics, Stockholm, Sweden

ARTICLE INFO

Article history:
Received 5 September 2012
Received in revised form
21 March 2013
Accepted 22 March 2013
Available online 23 April 2013

Keywords:
Sea ice
Models
Proxy records
Benchmarking
LGM
Holocene
Past millennium

ABSTRACT

A dominant characteristic of the available simulations of past sea ice changes is the strong link between the model results for modern and past climates. Nearly all the models have similar extent for pre-industrial conditions and for the mid-Holocene. The models with the largest extent at Last Glacial Maximum (LGM) are also characterized by large pre-industrial values. As a consequence, the causes of model biases and of the spread of model responses identified for present-day conditions appear relevant when simulating the past sea ice changes. Nevertheless, the models that display a relatively realistic sea-ice cover for present-day conditions often display contrasted response for some past periods. The difference appears particularly large for the LGM in the Southern Ocean and for the summer ice extent in the Arctic for the early Holocene (and to a smaller extent for the mid-Holocene). Those periods are thus key ones to evaluate model behaviour and model physics in conditions different from those of the last decades. Paleoclimate modelling is also an invaluable tool to test hypotheses that could explain the signal recorded by proxies and thus to improve our understanding of climate dynamics. Model analyses have been focused on specific processes, such as the role of atmospheric and ocean heat transport in sea ice changes or the relative magnitude of the model response to different forcings. The studies devoted to the early Holocene provide an interesting example in this framework as both radiative forcing and freshwater discharge from the ice sheets were very different compared to now. This is thus a good target to identify the dominant processes ruling the system behaviour and to evaluate the way models represent them.

1. Introduction

Sea ice is an important component of the climate system. Two of its main characteristics, namely the high albedo, and the low thermal conductivity, are associated with powerful feedbacks that generally amplify the climate variability at high latitudes. The one that is the most studied is the temperature-albedo feedback in which an initial warming (alternatively cooling) induces a decrease (increase) in the ice extent and thus in the albedo leading to a larger (lower) absorption of incoming solar radiation and finally an additional warming (cooling) (Ebert and Curry, 1993; Qu and Hall, 2006; Perovich et al., 2007; Flanner et al., 2011). This mechanism has significantly contributed to the recent decrease of the ice extent in summer in the Arctic (Perovich et al., 2007, 2008; Flanner et al., 2011). As sea ice isolates the ocean and the atmosphere, a decrease in the ice extent or in the ice thickness, due for instance to an initial atmospheric warming, will induce a larger heat transfer from the relatively warm ocean to the atmosphere in autumn and winter and then a prolonged warming of the atmosphere (the conduction feedback). In addition, for thinner ice, the ocean will cool faster and sea ice formation will be more rapid, partly compensating the initial decrease in ice extent (e.g., Ebert and Curry, 1993; Bitz and Roe, 2004).

Sea ice changes also affect the atmosphere and the ocean state, leading to both positive and negative feedbacks. Recent studies analysing the impact of the minima of summer sea ice extent between 2006 and 2008 in the Arctic suggest that the sea ice retreat has increased the humidity and modified stability of the atmospheric boundary layer. This induced a greater low cloud formation over newly opened water in early fall, reducing the surface heat losses by increasing the downward longwave radiation but also limiting the surface solar radiation (cloud-ice feedback; e.g., Kay and Gettelman, 2009; Kay et al. 2011). When sea ice forms, a part of the salt contained in seawater is rejected towards the ocean. This

* Corresponding author. Tel.: +32 10 47 32 98; fax: +32 10 47 47 22.
E-mail address: hugues.goosse@uclouvain.be (H. Goosse).

0277-3791/$ – see front matter © 2013 Elsevier Ltd. All rights reserved.
http://dx.doi.org/10.1016/j.quascirev.2013.03.011

process, which tends to destabilise the surface layer and to induce a deepening of the surface mixed layer, is a key element of the formation of deep water, in particular along the Antarctic continental shelf. In regions where the stability of the pycnocline below the mixed layer is low and where the water is relatively warm at depth, this mixed layer deepening brings thermal energy to the surface that tends to moderate further ice formation (Martinson, 1990; Martinson and Steele, 2001).

In addition to its active role in climate variations, sea ice is a sensitive diagnostic of any climate change. Because of its low inertia, related to its small thickness compared to the ocean and atmosphere, any change in the winds, in ice-ocean or atmosphere-ocean heat fluxes has indeed a large imprint on the ice cover. Furthermore, the shift from an ice covered to an ice free ocean is a clear modification of the system, easy to represent and to quantify even for non-specialists. The sea ice changes are thus among the most spectacular ones of the climate system, as illustrated by the attention received by the decrease in summer sea ice extent in the Arctic over the last decade (e.g., Parkinson et al., 1999; Comiso and Nishio, 2008; Stroeve et al., 2012).

This interest in sea ice has attracted modelling studies for more than 40 years (e.g. Maykut and Untersteiner, 1971; Semtner, 1976; Hibler, 1979; Parkinson and Washington, 1979) leading to large improvements over the years and major successes. However, the current results of the sea ice components of coupled climate models still have clear biases for present day-conditions. On average over the ensemble of available simulations, models are able to reproduce adequately the mean ice extent in summer and winter. This averaging, however, hides the large scatter between individual simulations that reaches several millions square kilometres (Arzel et al., 2006; Parkinson et al., 2006; Massonnet et al., 2012; Zunz et al., 2013). Models have more troubles to reproduce the variance of the system and the observed trends over the last decades, although some models are clearly more realistic than the others (Arzel et al., 2006; Parkinson et al., 2006; Stroeve et al., 2007; Massonnet et al., 2012; Zunz et al., 2013).

The model–data comparison focussing on the last decades is the main step in model evaluation since it is the period with the largest amount of precise observation. For instance, reliable estimates of the sea ice concentration based on satellite data start in the late 1970s only (Gloersen et al., 1999; Parkinson et al., 1999; Comiso and Nishio, 2008; Cavalieri and Parkinson, 2012; Parkinson and Cavalieri, 2012). This corresponds to a short sample that is insufficient to estimate the internal variability of the system on a wide range of timescale and to measure the influence of various forcings, in particular of forcing displaying a larger magnitude than the recent ones. Over the last decades, the sea ice extent in summer has strongly decreased in the Arctic. This trend is a combination of the response to forcing changes and the internal variability of the system but the exact contribution of each component could not be determined using recent observations. Furthermore, the time history of the forcing is complex and not precisely known. It is thus not possible to test adequately the impact of a forcing change in models on the basis of this period only, with a clear impact on the uncertainty in the projections of the state of the ice cover during the 21st century and beyond.

A complementary method for model evaluation is to perform simulations over most distant periods and to compare them with proxy records. The advantages are the longer time series, allowing for instance to analyse centennial changes, and the wide range of conditions. This also provides the opportunity to study mechanisms that are not dominant in the recent development of the sea ice cover but played a central role in the past and maybe again in the future. On the other hand, some forcings are more uncertain as we go back in time and the proxy records allow the reconstruction of a smaller number of climatic variables than modern instruments. Furthermore, as the proxies provide only indirect estimates of climate changes, it is necessary to transfer the recorded signal into the physical variables of the model such as the ice concentration or to include additional variables in the model to simulate directly the variable measured in the archives. The first method is the most widely applied but it is associated with many sources of uncertainties (see for instance the other papers in this special issue) inducing potential limitations in model–data comparison (e.g., Lohmann et al., 2012). The second one is more precise but requires significant model-development. It is relatively mature for some variables like the water isotopes (e.g., Roche et al., 2004; Schmidt et al., 2007; Sime et al., 2008) but not yet for sea ice related proxies.

Here, a brief overview of the modelling of past sea ice changes is provided. We focus on the last 20 ka, in particular on the time periods selected in the framework of the Paleoclimate Model Intercomparison Project (PMIP, e.g. Braconnot et al., 2007a) as they are the ones for which the largest amount of information can be obtained. Depending on the availability of the data and of previous analyses, the present review is based on simulations from PMIP2 and PMIP3 (which was coordinated with the more general exercise CMIP5, Couple Model Intercomparison Project, phase 5) as well as on experiments performed outside of those intercomparison exercises. The goal is not to be exhaustive on any particular time period or process as specific studies are required for this purpose. We rather present some examples illustrating how the simulation of past sea ice changes can be used to evaluate climate models as well as to analyse feedbacks and mechanisms in which sea ice plays a central role, presenting the current status of the field and the opportunities. The modelling of biogeochemical process is not discussed as it is the subject of another paper in this special issue.

Section 2 provides a short introduction to sea ice modelling. For more details, the readers should consult the description of recent models (e.g., Vancoppenolle et al., 2009; Hunke and Lipscomb, 2010) or a review specifically devoted to the subject (e.g., Hunke et al., 2010). Section 3 is focussed to the two most classical time periods analysed in PMIP: the mid-Holocene (6 ka BP) and the Last Glacial Maximum (LGM, 21 ka BP). Section 4 deals with transient runs covering the Holocene and more specifically the last millennium. In Section 5, we propose a discussion of two specific points: the perspectives in model–data comparison as well as the causes of model biases and of the spread in model results. Finally, some conclusions are presented.

2. Sea ice modelling

Sea ice is a highly heterogeneous medium made of individual ice floes whose size ranges from one metre to tens of kilometres. The ice thickness of first year sea ice (the ice which formed during the previous fall and winter) is typically of the order of one–two metres while multiyear ice (the one that had survived one summer at least) is generally between 2 and 4 m for present-day conditions. However, because of convergences and divergences in the pack, the sea-ice thickness can widely vary between a ridge of more than 10 m and open water (also termed lead) on a short horizontal scale. The sea ice itself includes brines and different types of ice crystals depending on the mechanisms leading to its formation. All those characteristics influence the behaviour of sea ice and its response to forcings. The goal of sea-ice models is to represent them as accurately as possible at the model-scale (Fig. 1), which is presently of the order of one hundred of kilometres or more for climate studies.

Traditionally, the processes taken into account in models are divided into dynamics and thermodynamic ones. Sea ice dynamics includes the movement and deformation of the ice. In this framework, sea-ice is considered to be a two-dimensional continuum, i.e.

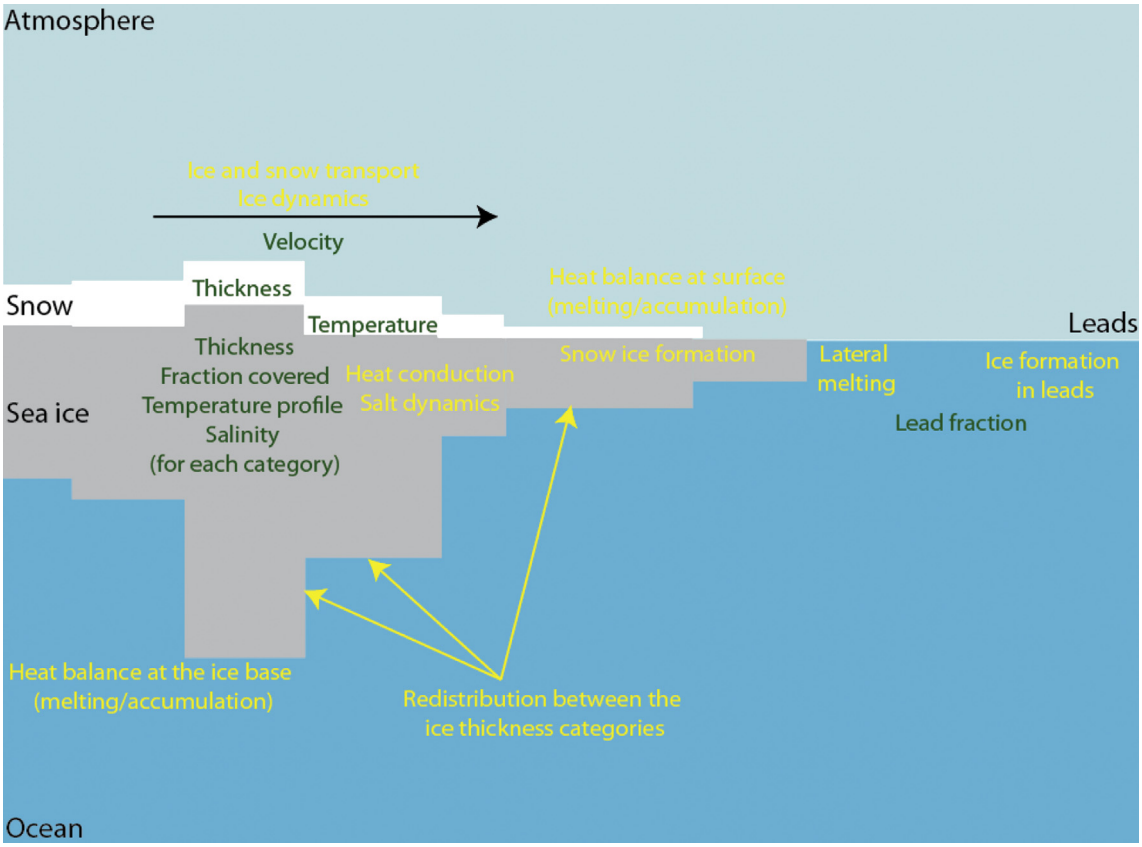

Fig. 1. Main variables (green) and processes (yellow) represented in a large-scale sea ice model.

that the model does not compute the velocity of each ice floe but an integrated velocity which characterizes the movement at the model grid-scale. This velocity is obtained by applying Newton's second law that relates the acceleration of the medium and the applied forces. When the pack is thin and/or the floe concentration is low, the dominant forces are the wind stress, the ocean stress and the Coriolis force. This case is usually referred as "free drift". The ice is generally driven by the winds and a classical rule of the thumb gives a sea ice velocity of about 2% of the wind speed at an angle of a few degrees to the right (left) of the wind in the northern (southern) hemisphere (e.g., Thorndike and Colony, 1982; Fukamachi et al., 2011). Inside the pack, when concentration and thickness are higher, internal ice stress plays a much larger role. It is given by a constitutive law that describes the characteristics of sea ice. The classical ones used in sea ice model are based on the viscous–plastic rheology of Hibler (1979) in which sea ice does not resist significantly to divergence because of the presence of cracks and leads in the pack but can oppose a large force to a convergent motion.

At large-scale, the vertical gradients of temperature are much larger than the horizontal ones and the dominant thermodynamic processes are occurring along the vertical. As a consequence, the thermodynamic part of the sea ice model is one-dimensional. It computes the heat balance at the interfaces with the ocean and the atmosphere, the sea ice melting/formation, as well as temperature profiles inside the ice in order to obtain the conduction flux. A fundamental characteristic of sea ice is that the conduction flux is strongly influenced by the ice thickness leading to a much larger ice formation in cold condition at the base of thin ice than at the one of thicker floes that efficiently isolates the ocean from the cold atmosphere (Maykut, 1982; Bitz and Roe, 2004). It is thus required to take into account the distribution of the ice between various thicknesses inside the model grid cell to have a fair estimate of freezing and melting rates. Representing the pack by a slab of sea ice of uniform thickness and leads that each occupies a fraction of the cell is a useful simplification, still made in several climate models, but this is a strong approximation that leads to clear biases in the models response to forcing (e.g. Holland et al., 2010; Massonnet et al., 2011). Snow also has a large insulating capacity, in addition to its specific radiative properties, characteristics that are taken into account using simple or more complex schemes (e.g., Lecomte et al., 2011).

It is important to note that this classical distinction between dynamical and thermodynamical processes is only formal. On the one hand, the ice dynamics strongly influences the ice thickness distribution, the formation of leads, etc, and thus the heat exchanges with the ocean and the atmosphere. The transport of sea ice towards lower latitudes where it meets warmer waters and melts is a central element of the mass balance of the sea ice system. On the other hand, the strength of the ice and its dynamical behaviour depend critically on the ice thickness and thus on the thermodynamical processes.

In order to resolve the processes mentioned above, some additional variables can be computed. The heat capacity, the latent heat and the conductivity of the ice are a function of its salinity that is now explicitly included in some models (e.g., Vancoppenolle et al., 2009). The fraction of the surface covered by melt ponds collecting the freshwater due to melting provides essential information for an accurate estimate of the surface albedo (e.g., Flocco et al., 2010), whose value is critical for the absorption of solar radiation and thus on surface melting. Alternatively, the characteristics of the ice such as its albedo can be parameterized in a simpler way, i.e. deduced

from existing model variables like the ice thickness and the state of the surface (melting or non-melting). Many additional processes (the effect of flooding of the snow layer by seawater when the snow ice interface is below the water level leading to the formation of snow ice, the ridging induced by convergence, etc) are also represented through parameterizations for which various methods and level of sophistication are applied.

The models differ thus not only in the choice of the processes and variables that are represented but also in the way the parameterization are applied. The models used for the simulations of past climates in the framework of PMIP3 are the same as the ones applied for present and future changes in CMIP5. Consequently, the majority of them include relatively sophisticated sea ice components. However, the models used in paleoclimatology for long transient simulations or for ensemble of simulations are often Earth Model of Intermediate Complexity (EMICs) or older generation models that incorporate a more simplified approach in order to be less computer-time demanding, as discussed below (Table 1).

3. Snapshots: 6 ka BP and LGM

The changes in forcing from the pre-industrial climate to 6 ka BP result in more incoming solar radiation during northern hemisphere summer, and less insolation during the northern hemisphere winter, the changes in summer being larger than the ones in winter (Berger and Loutre, 1991). As discussed recently in Berger et al. (2013), confirming earlier studies (e.g., Otto-Bliesner et al., 2006; Braconnot et al., 2007b; Fischer and Jungclaus, 2011), the response of all the models to the increase in summer insolation is similar and characterized by a decrease in summer (minimum) sea ice extent at 6 ka BP in the northern hemisphere as compared to the pre-industrial conditions (Fig. 2). In the majority of the models, this decrease is smaller than $1 \cdot 10^6$ km^2 but reaches more than $2 \cdot 10^6$ km^2 in some of them (BCC-CSM1-1, CNRM-CM5, HadGEM2-CC, HadGEM2-ES, MRI-CGCM3). Changes in greenhouse gas concentration is also included as a forcing in the majority of the models but its role is generally less important than the one of insolation (e.g., Braconnot et al., 2007a; Renssen et al., 2009).

Table 1
Summary of the model simulations[a] that are shown in the present study.

Model	Modelling center	Resolution of the sea ice model[b]	Main components of the sea ice model[c]	References	Period simulated
BCC-CSM1-1	Beijing Climate Center, China	(1°–1/3°) × 1°	ITP, EVP	http://www.lasg.ac.cn/C20C/UserFiles/File/C20C-xin.pdf	6 ka BP
CCSM3	National Centre for Atmospheric Research (NCAR), USA	0.3°–1° × 1°	ITD, EVP	Otto-Bliesner et al. (2006)	LGM; 6 ka BP
CCSM4		~0.6° × 0.9°	ITD, EVP	Gent et al. (2011)	Last Millenium; 6 ka BP, LGM
CNRM-CM3	Centre National de Recherches Météorologiques, France	~0.5–2° × 2°	ITD, EVP	Salas-Mélia et al. (2005)	LGM
CNRM-CM5		~1/3°–1° × 1°	ITD, EVP	Voldoire et al. (2012)	6 ka BP, LGM
CSIRO-1.0	Commonwealth Scientific and Industrial Research Organization, Australia	R21 (~3.2° × 5.6°)	No ITD, CV	Phipps (2006)	6 ka BP
CSIRO-1.1					
CSIRO-Mk3.6		T63 (~1.9° × 1.9°)	No ITD, CV	Rotstayn et al. (2012)	6 ka BP
CSIRO-1.2		R21 (~3.2° × 5.6°)	No ITD, CV	Phipps et al. (2011)	6 ka BP
ECBILT-CLIO	Koninklijk Nederlands Meteorologisch Instituut, Netherlands	3° × 3°	No ITD, VP	Renssen et al. (2005a, 2005b) Renssen et al. (2009)	LGM; 6 ka BP Last 9 ka BP
ECHAM5/MPI-OM	Max-Planck-Institut für Meteorologie, Germany	T30 (~3° × 3°)	Virtual ITD, VP	Fischer and Jungclaus (2011)	Last 6 ka BP
FGOALS-1.0g	LASG, Institute of Atmospheric Physics, China	1° × 1°	ITD, EVP	Yu et al. (2004)	LGM; 6 ka BP
FGOALS-s2		0.5°–1° × 1°	ITD, EVP	http://www.lasg.ac.cn/FGOALS/CMIP5	6 ka BP
FOAM	Centre for Climatic Research, USA	2.8° × 1.4°	No ITD, no dynamics	Jacob et al. (2001)	6 ka BP
GISS-E	NASA Goddard Institute for Space Studies, USA	4° × 5°	No ITD, VP	Schmidt et al. (2006)	6 ka BP
HadCM3M2	Met Office, UK	1.25° × 1.25°	No ITD, simplified dynamics	Johns et al. (2003)	LGM
HadGEM2-CC		0.3–1.0° × 1°	ITD, EVP	Martin et al. (2011)	6 ka BP
HadGEM2-ES			ITD, EVP		6 ka BP
IPSL-CM4-V1-MR	Institut Pierre Simon Laplace des Sciences de l'Environnement, France	~0.5°–2° × 2°	Virtual ITD, VP	Marti et al. (2005)	LGM
IPSL-CM5A-LR		~0.5°–2° × 2°	Virtual ITD, VP	http://icmc.ipsl.fr/	6 ka BP
LOVECLIM1.1	Georges Lemaître Centre for Earth and Climate Research, Belgium	3° × 3°	No ITD, VP	Goosse et al. (2010), Roche et al. (2012)	LGM
LOVECLIM1.2				Goosse et al. (2007) Crespin et al. (2013)	Last 8 ka BP Last Millenium
MIROC3.2	Japan Agency for Marine-Earth Science and Technology, University of Tokyo, National Institute for Environmental Studies	0.5° × 1.4°	No ITD, EVP	K-1-Model-Developers (2004)	6 ka BP; LGM;
MIROC-ESM		~1° × 1.4°	No ITD, EVP	Watanabe et al. (2011)	6 ka BP, LGM
MPI-ESM E1/E2	Max-Planck-Institut für Meteorologie, Germany	From 22 km to 350 km.	Virtual ITD, VP	Jungclaus et al., 2010	Last Millenium
MPI-ESM-P		0.8° × 1.4°	Virtual ITD, VP	Raddatz et al. (2007), Marsland et al. (2003)	Last Millenium 6 ka BP, LGM
MRI-CGCM2-fa	Meteorological Research Institute Japan	2.5° × 0.5°	No ITD, simplified dynamics	Yukimoto et al. (2006)	6 ka BP
MRI-CGCM2-nfa					
MRI-CGCM3		~1.4° × 1°	No ITD, VP	http://www.mri-jma.go.jp/Publish/Technical/DATA/VOL 64/tec rep mri 64.pdf	6 ka BP, LGM
UBRIS	Met Office Hadley Centre, UK	1.25° × 1.25°	No ITD, simplified dynamics	Gordon et al. (2000)	6 ka BP

[a] The information about models is based on available information at the time of writing. For some models, additional information is posted on the CMIP5 website (http://cmip-pcmdi.llnl.gov/cmip5/).
[b] As many models use a complex grid, the numbers are indicative only.
[c] ITD = Ice Thickness Distribution, EVP = Elasto-plastic rheology, CV = cavitating fluid rheology, VP = Visco-plastic rheology, simplified dynamics = sea ice transport derived from ocean velocity.

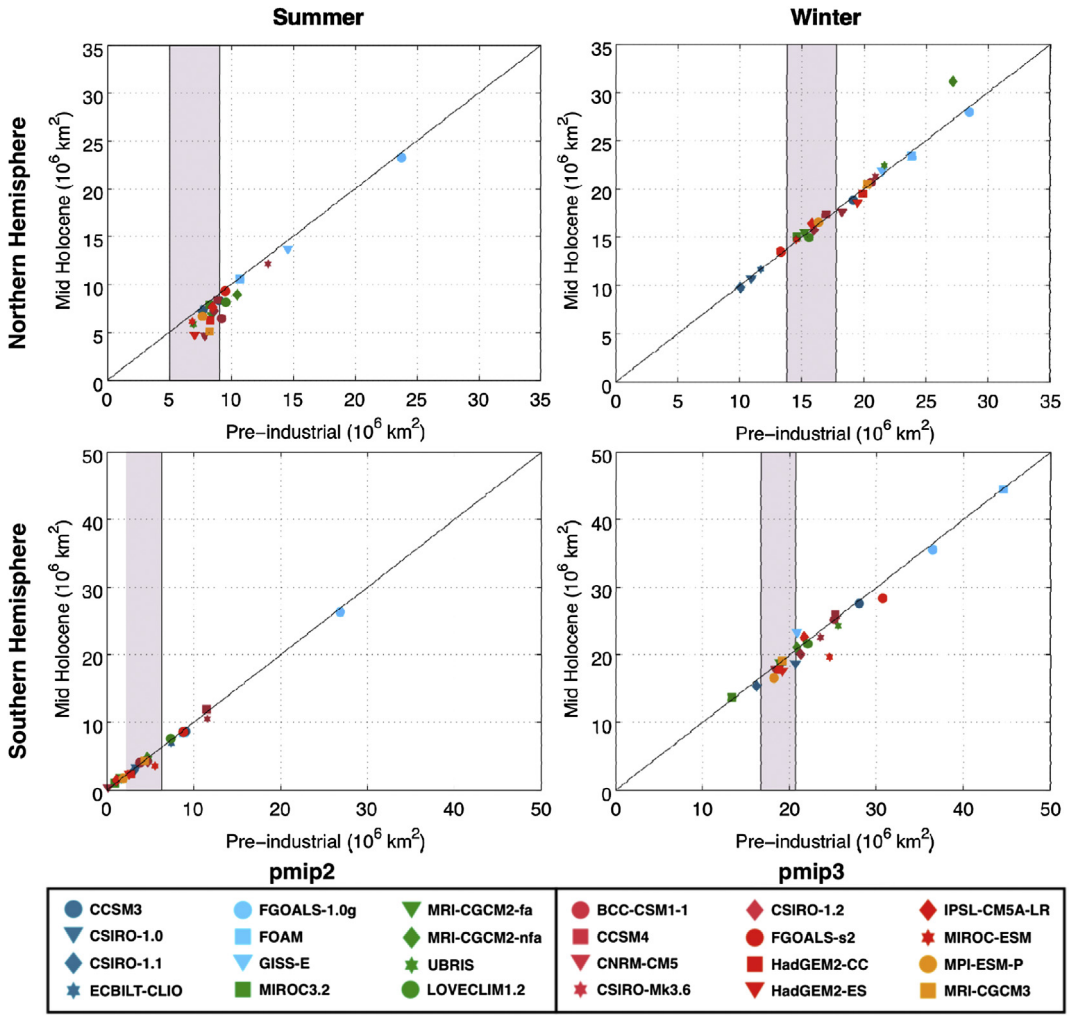

Fig. 2. Simulated ice extent at 6 ka BP during the month of minimum (summer) and maximum (winter) ice extent in northern and southern hemispheres as a function of the pre-industrial value. The observations based on satellite data for the period 1979–2000 with a range of $2 \cdot 10^6$ km^2 are given in grey shading (Fetterer et al., 2012). A difference between satellite data and pre-industrial values is expected (see Fig. 7, Goosse et al., 2012) but this difference is smaller than the mean model bias and smaller than the range of $2 \cdot 10^6$ km^2 displayed. The models corresponding to blue and green colours are from PMIP2, the ones with red and orange colours are from PMIP3.

For the winter sea ice cover, the changes are generally weaker and the models are not as consistent: about 3/4 of the models simulate a slightly reduced maximum sea ice cover at 6k as compared to the maximum pre-industrial ice cover. It means that in those models, the decrease in ice extent and lower ice thickness in summer (see below) allow a larger heat storage in the system, heat that is released in autumn and winter and is able to overwhelm the effect of a lower insolation during this period of the year at 6 ka BP. The rest of the models simulate a more extensive maximum sea ice cover in 6 ka BP as a more direct response to insolation changes during this part of the year.

In the southern hemisphere, the scatter between the models is larger but this mainly reflects the biases in the pre-industrial conditions: the difference in the simulated sea ice cover between the control climate and 6 ka BP are small for all models, the ice extent being only slightly reduced in the majority of models in the 6k simulations, both for the maximum and minimum ice cover. Renssen et al. (2005b) argue that this smaller ice extent is due to the higher insolation in winter and spring that directly induced higher temperatures during those seasons. Furthermore, because of the memory of the system, which keeps the influence of those warmer conditions through a reduced ice extent and ice thickness as well as through heat storage in the top layers of the ocean, this signal propagated to the other seasons.

Those results illustrate that, for the same model, the simulated sea ice extents are not very different for 6 ka BP and pre-industrial conditions. Berger et al. (2013) discussed actually that, in the Arctic, the change in the sea ice thickness from the 6 ka BP to the pre-industrial climate is more prominent in all PMIP2 models than the changes in sea ice extent: the simulated sea ice cover becomes thinner in the mid-Holocene simulations compared to the control, for all models and all seasons (preliminary analyses confirm this result for PMIP3 simulations). As a consequence, the way a model simulates the sea ice extent at 6 ka BP does not bring a lot of new information about its relative skill at high latitudes in regards to what is brought by the model–data comparison for the modern period which is based on more precise observations. More subtle diagnostics are thus required to get the best of those past simulations. It is however instructive to see that all the models that display a larger decrease in the sea ice extent in summer in the Arctic are coming from the PMIP3 archive. This can be related to the conclusion that recent models included in the CMIP5 archive simulate on average a larger decrease in summer sea ice extent for the recent decades than the older model versions in CMIP3 (Massonnet et al., 2012; Stroeve et al., 2012).

Because of this link between mid-Holocene and modern conditions, only the models that display a reasonable ice extent for present-day conditions have been shown in Fig. 3. To be selected, the mean ice extent of the model has to be within $2 \cdot 10^6$ km^2 of the observations for modern conditions for both seasons. As many models are better in one hemisphere compared to the other, different models can be chosen for the Arctic and the Southern Ocean. Many methods have been proposed to identify the "best models" (e.g., Massonnet et al., 2012; Wang and Overland, 2012) but there is no objective and general rule than could be applied in all cases. No model is better than the other ones in all the regions, for all the variables (mean and variance of the ice concentration, of the ice thickness, etc). Furthermore, to identify the robustness of processes among a wide range of conditions, it can be wiser to take into account all the available models including the ones that have a biased mean state but a different representation of some relevant mechanisms. The $2 \cdot 10^6$ km^2 limit should thus certainly not be considered as a strong choice but rather as a way to illustrate the behaviour of a few models only among all the available ones in the present overview.

The models included in PMIP2 (Berger et al., 2013) display a winter ice edge location on the western side of the Atlantic located from the northern part of the Greenland coast in the north, to Newfoundland in the south. On the eastern side, the PMIP2 models can be divided in two groups, one for models with the sea ice edge located in the Barents Sea (CCSM3, CSIRO1.0, CSIRO1.1, ECBILT-CLIO, GISS-E, MIROC3.2, MRI-CGCM2-fa, and UBRIS) and the other for models with the ice edge extending all the way south to the Great

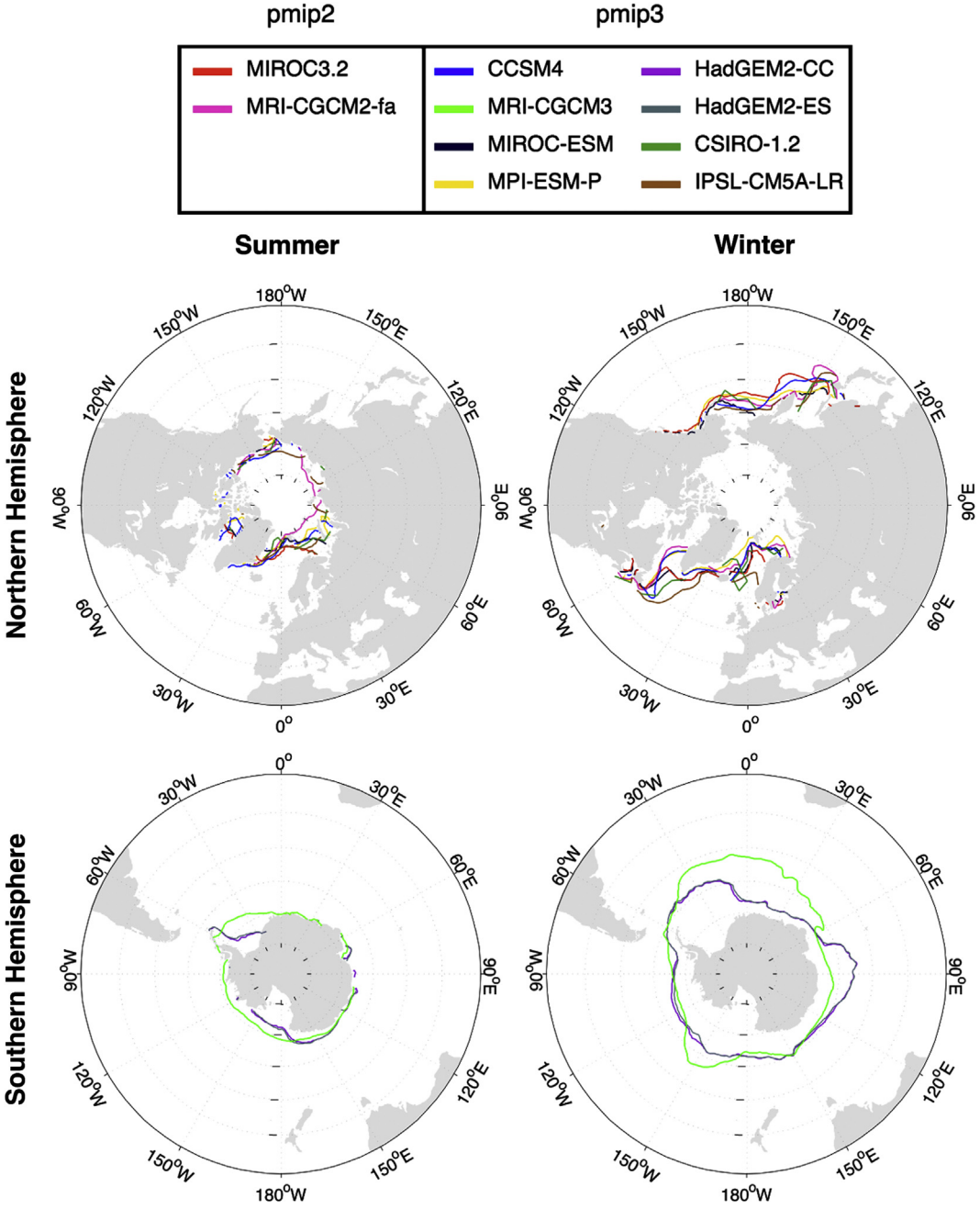

Fig. 3. Location of the ice edge, defined as the 15% concentration limit at 6 ka BP in summer and winter (March and September) for a selection of models that display for present-day conditions ice extent within $2 \cdot 10^6$ km^2 of observations for both seasons in each hemisphere (see Fig. 2).

Britain (FGOALS-1.0g, FOAM, and MRInfa), reflecting the model behaviour for present-day conditions (Berger et al., 2013). If we restrict the analysis to the models included on Fig. 3, the range of the model is much smaller and relatively close to present-day conditions with some models like IPSL-CM5A-LR showing a large ice extent in the western Atlantic and some others in the North Pacific as MIROC3.2.

In summer, while the extent displays a very wide range if all the models are analysed (Berger et al., 2013), the ice remains only in the central Arctic in the models selected for Fig. 3. Proxy data based on drift wood and beach ridge formation indicate that the sea ice along the East Greenland reached a minimum sometimes between 8.5 and 6 ka BP, with the summer ice edge limit located at 83°N, approximately 1000 km north of present day ice limit (Funder et al., 2011). Only a few models (e.g., MRI-CGSM2-fa) simulate the summer sea ice edge at such high latitude suggesting an underestimation of the response to the forcing in this region in some models.

Fig. 3 also illustrates some of the limitations of our selection criteria which is based on the ice extent over the whole hemisphere as some models display a too large extent in one sector that is compensated by an underestimation in another one. This is particularly critical in the Southern Ocean where, in winter, HadGEM2-CC and HadGEM2-ES underestimate the ice extent in the eastern Weddell Sea but overestimate it in the Pacific sector. In summer, all the models in Fig. 3 have a reasonable mean extent by definition but a too high ice concentration in the Ross Sea and a too low in the Bellingshausen Sea. By contrast, some models with a good representation of the ice the Bellingshausen Sea but a similar or weaker overestimation in the Ross Sea have a net bias on the mean ice extent and are thus not included in Fig. 3 following our very simple selection criteria.

In order to simulate conditions corresponding to the LGM, the PMIP2 and PMIP3 protocols recommend to modify the ice-sheet topography and albedo following the global ice sheet reconstruction ICE-5G described in Peltier (2004) in PMIP2 and a blending of three different sources for PMIP3 (http://pmip3.lsce.ipsl.fr/), to change the concentration of CO_2, CH_4 and N_2O, and to impose astronomical configuration corresponding to 21 ka BP in the computation of the insolation (Berger, 1978). In response to those changes, the models consistently simulate an equatorward expansion of the sea-ice cover at the LGM compared to the pre-industrial state, as expected in a colder, glacial, climate (e.g., Hewitt et al., 2003; Otto-Bliesner et al., 2006; Braconnot et al., 2007b; Roche et al., 2007, 2012). One has to be careful that this does not necessary induce a larger surface covered by sea ice compared to pre-industrial conditions because of the different land-sea masks leading to a smaller ocean surface at LGM, in particular in the Arctic (Fig. 4).

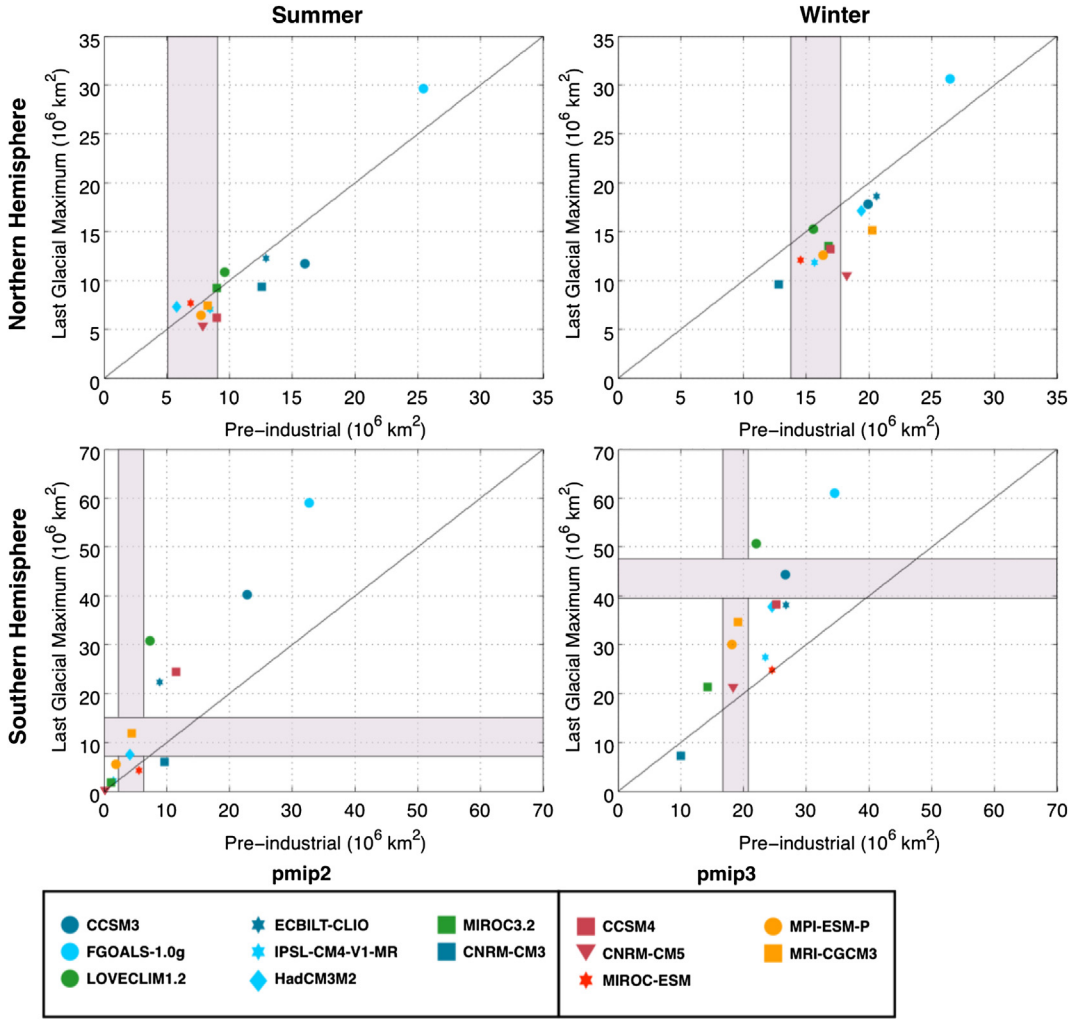

Fig. 4. Simulated ice extent at the LGM during the month of minimum (summer) and maximum (winter) ice extent in northern and southern hemispheres as a function of the pre-industrial value. The observations based on satellite data for the period 1979–2000 with a range of $2 \cdot 10^6$ km^2 (Fetterer et al., 2012) and the estimates of Roche et al. (2012) for the Southern Ocean are given in grey shading. The models corresponding to blue and green colours are from PMIP2, the ones with red and orange colours are from PMIP3.

As noticed for 6 ka BP, there is a link between the pre-industrial ice extent and the one simulated in each model at LGM but this link is much weaker than for 6 ka BP, in particular for the Southern Ocean. There, although nearly all models simulate a larger sea-ice cover for winter and summer under LGM conditions, the spread of the response is very large as detailed in the recent review conducted by Roche et al. (2012) for PMIP2 models. For the summer extent, model response ranges from models with only some coastal sea-ice around Antarctica to other ones with nearly $60 \cdot 10^6$ km^2. Besides, some models that agree reasonably well with observations for modern data, such as the MRI-CGCM3, are also close to the $11.1 \pm 4 \cdot 10^6$ km^2 value estimated by Roche et al. (2012) for this period using reconstructions based on proxy data. Similarly, the winter sea-ice edge is found in models between 40°S and 65°S, a spread of 25° in latitude (Roche et al., 2012). Broadly, data evidence shows a sea-ice edge between 55 and 50°S during LGM in winter (Gersonde et al., 2005). Consequently, the data limit is within the model spread and a few models are reasonably close to the value of $43.5 \pm 4 \cdot 10^6$ km^2 given by Roche et al. (2012) based on proxy evidence (CCSM3, CCSM4, ECBILT-CLIO, HADCM, MPI-ESM-P, MRI-CGCM3). Among those ones, a few such as MRI-CGCM3 are also close to observations in winter for modern conditions. However, all models are showing a fairly zonal sea-ice distribution around the Antarctic continent, in disagreement with data evidences showing a more oval shaped distribution (Gersonde et al., 2005), with maximum sea-ice expansion in the Atlantic sector of the Southern Ocean (Fig. 5; Roche et al., 2012). Additionally, Roche et al. (2012) showed that the seasonal range in sea-ice at the LGM is very close to the pre-industrial one in the PMIP2 models, a fact at odds with data evidences that calls for increased seasonality. Although some models show a somehow larger amplitude of the seasonal cycle at LGM like MRI-CGCM3 and MPI-ESM-P, this bias appears valid to a large extent for the PMIP3 models analysed here.

In the eastern North Atlantic, the simulated sea-ice limit for the LGM in the PMIP2 and PMIP3 models in summer is located in the Nordic Seas in some models while it reaches Iceland in others. In the western North Atlantic, the summer ice edge is found anywhere between the southern tip of Greenland to the coast up to Newfoundland. This spread has some similarities with the one simulated for the pre-industrial winter within the same area and all the models selected for Fig. 5 have a relatively small ice cover in this sector. Turning to the North Pacific, only a few of the climate models considered are simulating a significant cover there. Among the ones included in Fig. 5, only MIRCO-ESM has some ice remaining in the Okhotsk Sea.

Comparing with proxy data is complicated in the North Atlantic because of contradicting evidences arising from different type of proxies. If dinocysts suggest largely ice free conditions during LGM summer in the Nordic Seas (de Vernal et al., 2000), foraminifera abundances indicate partial sea-ice cover with a strong East–West gradient from perennial sea-ice cover at the Greenland coast and ice-free conditions at the Norwegian coast (Kucera et al., 2005). The models are clearly in better agreement with the latter inferences, simulating in the majority of them a strong gradient between Greenland and Norway with a sea-ice limit between Iceland and Svalbard.

During winter, models are simulating a substantial increase in sea-ice extent with expansion of the sea-ice cover over much of the Nordic Seas and even to Scotland as well as a large increase in the western North Atlantic Ocean and in the eastern part of the Pacific (Fig. 5). In winter, the different proxies also indicate a large southward expansion of sea-ice along the American coast of the northern Atlantic Ocean and a likely large cover in the western Atlantic open ocean (de Vernal et al., 2000; Pflaumann et al., 2003). Proxy data suggests some winter sea-ice cover as well along the European coast up to at least southern Ireland. The models broadly agree with such a pattern, except for the too marked increase in sea-ice (up to 40°N) on the American side of the North Atlantic Ocean in some of them.

4. Transient changes: the Holocene and the last millennium

In addition to the quasi-equilibrium simulations using fixed boundary conditions such as the ones discussed in the previous section, transient simulations are now regularly performed, in particular for the Last Interglacial, the last deglaciation and the Holocene (e.g., Crucifix and Loutre, 2002; Calov et al., 2005; Timmermann et al., 2009; Smith and Gregory, 2012). For the Holocene, models are generally driven by orbital forcing and changes in greenhouse gas concentrations. In response to those forcings, the simulated sea ice developments in summer and winter are monotonic over the past six to eight thousand years (Renssen et al., 2005a, 2005b; Fischer and Jungclaus, 2011; Fig. 6). It means that the analysis of conditions at 6 ka BP gives a good qualitative overview of the major characteristics of Holocene change. The amplitude of the changes is, however, larger for the early Holocene than for 6 ka BP, which is consistent with the larger forcing. As a consequence, the difference between the results of different models or between simulations performed with the same model but using different parameters are clearer, which allows an easier distinction between the simulations that are in agreement or not with the proxy based reconstructions (e.g., Goosse et al., 2007). This comparison is nevertheless not straightforward because of the relatively small number of proxy available to describe the complex structure of the changes but also as the variability of the system as well as changes in the mean state are expected when sea ice extent is reduced in the Arctic, with a potential impact of the interpretation of the proxies (Goosse et al., 2009; Lohmann et al., 2012; Berger et al., 2013).

When the influence of the remnant Laurentide ice sheet on the surface albedo, topography and freshwater discharge are also included as forcing for the Early Holocene, a cooling at high latitudes of both hemispheres is simulated (Renssen et al., 2009, 2010, 2012). As a consequence, the ice extent in summer displays a minimum around 8 ka BP in summer, about 1000 years later in winter. In the northern hemisphere, this cooling, which agrees well with observations (Renssen et al., 2009), is directly due to the local temperature changes associated with higher elevation and a decreased absorption of solar radiation over Eastern Canada as well as to a moderate reduction of the meridional overturning circulation in the North Atlantic which then transports less heat northward. As a consequence, the largest increase in sea ice extent in response to those forcings is located in the western North Atlantic. In the Southern Ocean, the larger sea ice extent in response to Laurentide Ice Sheet deglaciation in the simulations of Renssen et al. (2010) is caused by the transport and upwelling in this region of colder deep water formed in the Atlantic. This advective link between the two hemispheres provided by the ocean circulation implies that they both cool more or less at the same time, in contrast to the seesaw between the two hemispheres obtained in many models when a larger freshwater flux is applied in the North Atlantic, inducing a major reduction of the meridional overturning circulation (e.g., Stocker, 2002; Stouffer et al., 2005).

Compared to the transient simulations covering the whole Holocene, the experiments focussing on the past millennium include additional natural (solar, volcanic) and anthropogenic forcings (greenhouse gases, aerosols, land-use changes) (e.g. Schmidt et al., 2011). In both hemispheres, the trend of the annual mean sea-ice extent is positive between 850 and roughly 1800, before a significant decrease (Fig. 7). In the majority of the models, this pre-

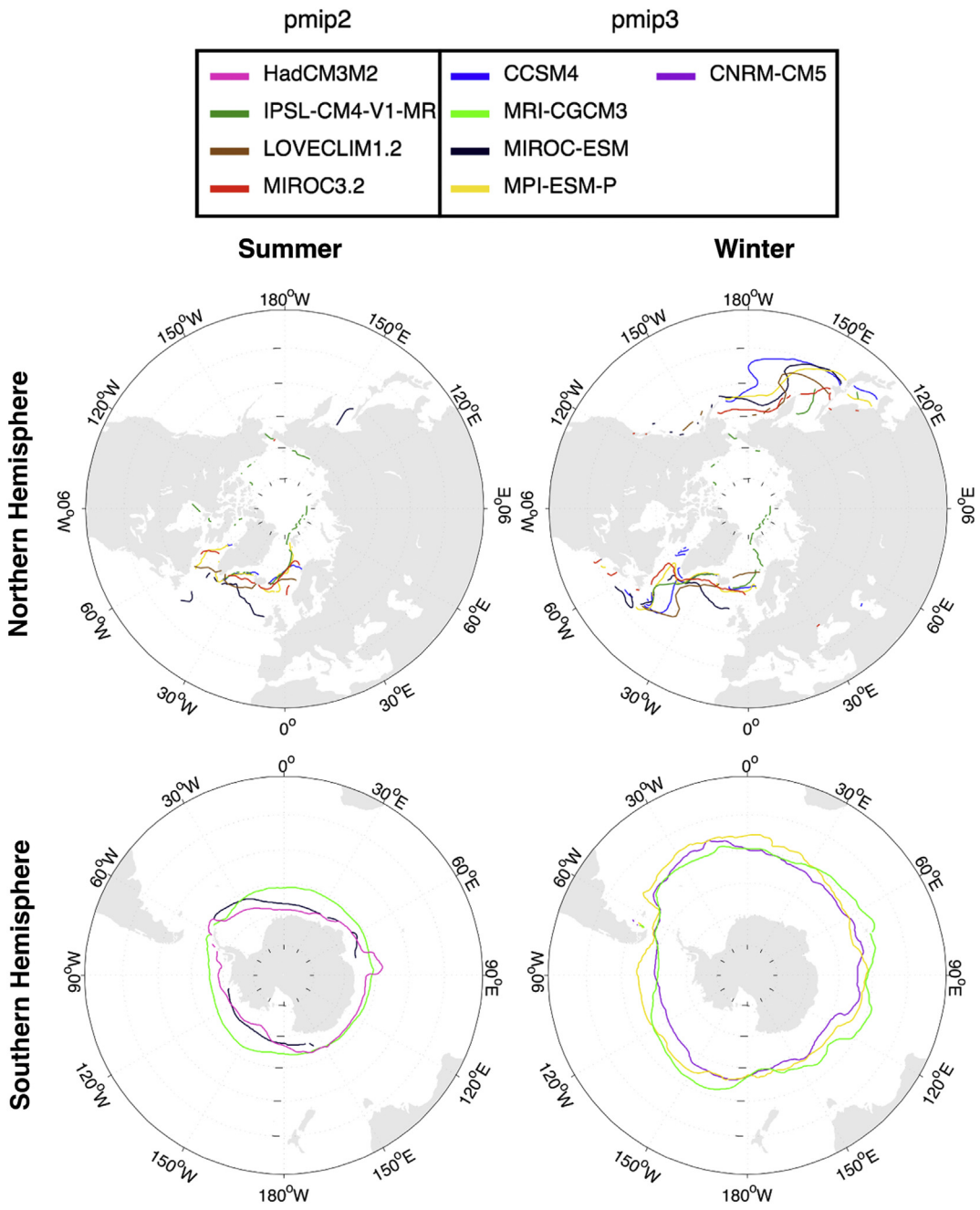

Fig. 5. Location of the ice edge, defined as the 15% concentration limit, at the LGM in summer and winter (March and September) for a selection of models that display for present-day conditions ice extent within 2 10^6 km^2 of observations (see Fig. 4). As only a few models are close to modern observations in the southern hemisphere among the ones that have available results for LGM, it is not imposed as for fig. 3 and the northern hemisphere that they have a low bias in both seasons but only in the season displayed (i.e. models should display reasonable ice extent for modern conditions in summer *or* in winter in the southern hemisphere not in summer *and* in winter as for the other panels). Present-day continental configuration is shown.

industrial trend is weaker in the southern hemisphere than in northern hemisphere. It can be viewed as being part of the general cooling trend simulated at high latitudes over the Holocene (Fig. 6). However, the forcings included in the addition to the orbital one, which is responsible for the changes at the scale of the Holocene, play also a role: although the surface cooling induced by the reduction of surface incoming radiation at surface after a major volcanic eruption lasts only a few years, the more intense volcanic activity associated with a higher number of large eruption between the 13th and 19th has clearly contributed to the long term cooling trend at high latitudes (Goosse et al., 2012; Miller et al., 2012; Crespin et al., 2013). Furthermore, Miller et al. (2012) identified a feedback involving sea-ice (Zhong et al., 2011) that amplifies the initial cooling induced by the volcanic eruption leading to a perturbation of the system that could last several decades. More surprisingly, some simulations suggest that the land-use change, which occurred at low and mid-latitudes and induce a global cooling over this period, may have a remote influence in Polar Regions (Goosse et al., 2012; Crespin et al., 2013). No large scale reconstruction exists for the southern hemisphere. For the northern hemisphere, the simulated trends are in qualitative agreement with the reconstruction of Kinnard et al. (2011), except during 17th

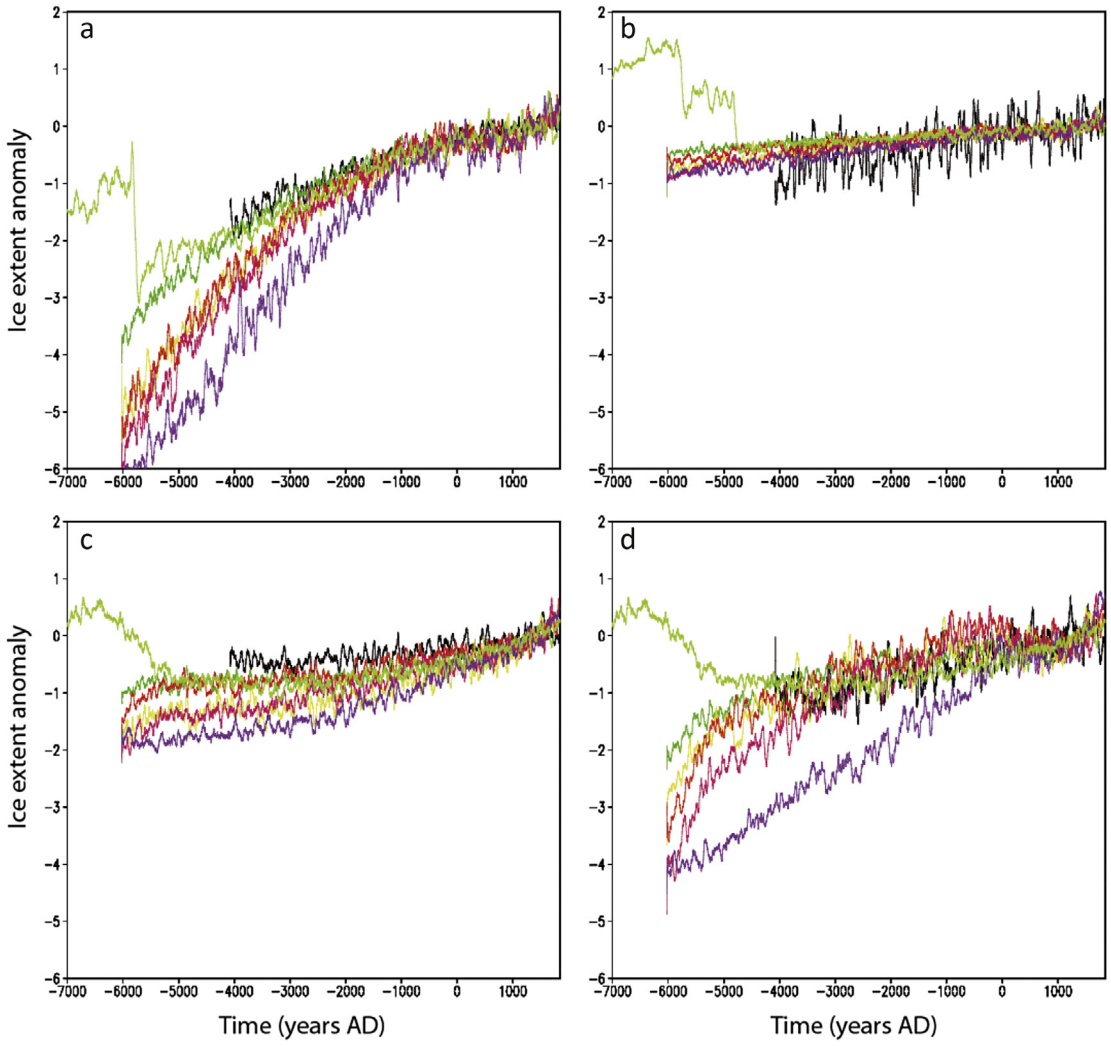

Fig. 6. Time series of the anomaly of ice extent (in 10^6 km^2) a) in the northern hemisphere in summer (September), b) in the northern hemisphere in winter (March), c) in the southern hemisphere in summer (March), d) in the southern hemisphere in winter (September). The results of ECHAM5/MPI-OM are in black (simulation covering the last 6000 years, Fischer and Jungclaus, 2011). Five simulations covering the last 8000 years with LOVECLIM1.1 using different model parameters are in green, yellow, red, magenta and violet (Goosse et al., 2007). The parameters that are varied are mainly related to the radiative scheme leading to climate sensitivities ranging from 1.6 to 3.8 K. An additional simulation with ECBILT-CLIO over the last 9000 years is in light green (Renssen et al., 2009). Compared to the other simulations, this longer simulation includes a forcing related to the presence of remains of the Laurentide during the early Holocene (effect on the surface albedo, elevation and freshwater forcing). Note that the plotted time series end in 1850 as some simulations does not include anthropogenic forcings. The reference period is 1000–1850 and a 51-year running mean has been applied to the time series.

and 18th century that are characterized by a local minimum in ice extent in the reconstruction while the simulated ice extent is close to its maximum. The surface air temperature reconstructions at high latitudes display cold conditions during that period (e.g. Kaufman et al., 2009), as also simulated by the models. As a consequence, low surface air temperatures and ice extent appear consistent in models while the reconstructions suggest a decoupling between the two, maybe related to modifications in oceanic exchanges between the Arctic and the North Atlantic.

5. Discussion

5.1. Some perspectives in model–data comparison

The qualitative or semi-quantitative comparisons of the results of different models with data and between them, such as the ones that have been performed up to now in the majority of the cases for sea ice, are instructive. They provide a more or less explicit ranking of the models related to the response in different regions (e.g. Roche et al., 2012; Berger et al., 2013) and in some cases attempts have been made to use this information in order to reduce the uncertainty on sea ice projections (e.g., Goosse et al., 2007). It is possible and suitable to go a step forward by performing more quantitative estimates of the model–data mismatch leading to a more objective evaluation of the models skill, through a specified metrics for instance. A few studies have followed this goal but this is, however, not yet systematic in paleoclimatology (e.g., Annan and Hargreaves, 2006; Schneider von Deimling et al., 2006; Edwards et al., 2007; Schmidt, 2010; Zhang et al., 2010; Hargreaves et al., 2011; Braconnot et al., 2012), and none of those studies were specifically focused on sea ice. A central issue is the interpretation of the various proxies and of their uncertainties as it has a large impact on the estimates of the reliability of model results (e.g. Hargreaves et al., 2011, 2012).

In the same framework, the goal of data assimilation is to optimally combine model results and proxy records to provide additional information on the past state of the system, on the processes responsible for the changes and on the model–data

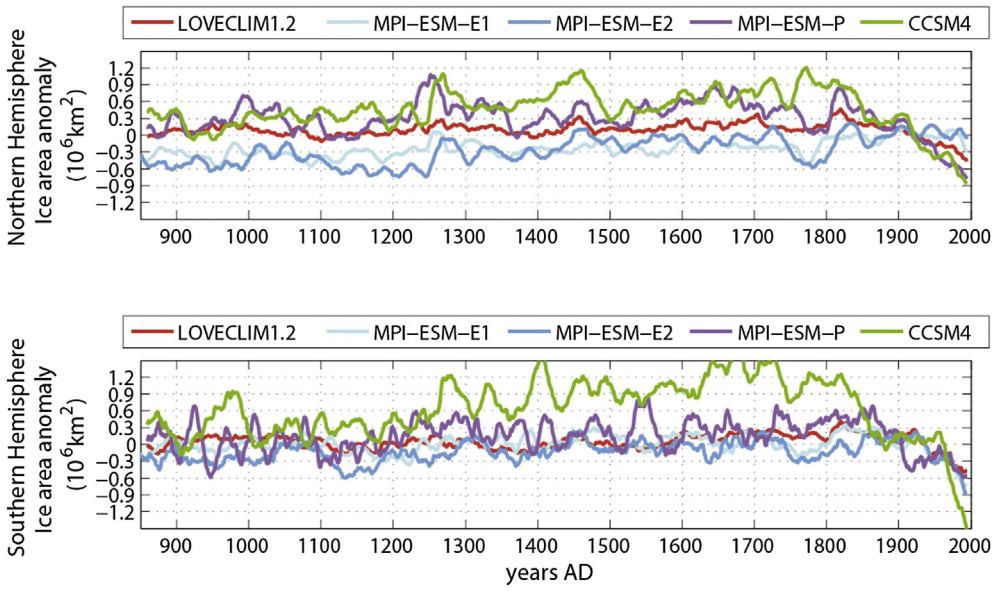

Fig. 7. Anomaly of annual mean sea ice area (in 10^6 km^2) simulated in five different models over the last millennium in the northern hemisphere and in the southern hemisphere. LOVECLIM1.2 results are in red, MPI-ESM-E1 in light blue, MPI-ESM-E2 in dark blue, MPI-ESM-P in violet, CCSM4 in green. The reference period is 1850–1980 AD and a 21-year running mean has been applied to the time series.

agreement. As this is technically obtained by constraining the model to be in agreement with proxy records, taking into account uncertainties in model results, forcing and proxies, it also requires a quantitative measure of the model–data differences. Data assimilation, which is now standard in many geophysical fields, has been applied in paleoclimatology too (see for instance the recent review of Widmann et al., 2010). However, the models were driven by reconstructions of surface temperature only, providing indirect information on sea ice (e.g., Goosse et al., 2012) but we can expect that, in the near future, simulations will be performed in which sea ice proxies, such as the one described in this special issue, are used in data assimilation experiments.

5.2. Potential causes of model–data and model–model discrepancies

In parallel to this quantitative evaluation of the model behaviour, it is also important to understand the causes of the model biases and of the spread in the different models responses to changes in the forcings. Actually, those two points appear somehow linked as several studies have related the decrease in the summer sea ice extent in the Arctic over the 21st century simulated by a model to its mean state for present or pre-industrial conditions (e.g., Zhang and Walsh, 2006; Holland et al., 2008; Boé et al., 2009a; Massonnet et al., 2012). As discussed in Massonnet et al. (2012), some of those relationships are due to simple physical mechanisms. Models with a smaller initial ice extent and smaller initial ice volume will need less energy to melt ice and will reach faster an ice free state. Similarly, models with a large area of thin ice generally display a faster decrease in the ice extent as the thin ice already melts for moderate warming. Models with a larger amplitude of the seasonal cycle also tends to simulate a faster decrease of the ice extent, likely because they are more sensitive to the forcing as illustrated for present-day condition by the response to the changes in solar insolation between summer and winter.

Similar arguments can then be applied to explain part of the spread of model responses during past periods. At the zero order, it has been shown in Section 3 that the biases in ice extent for present-day conditions are also generally seen for the past. Furthermore, all other factors being equal, models with lower ice volume or larger extent of thin ice will likely display a larger decrease in ice extent for past warm conditions. In this framework, the models that display the largest decrease of sea ice extent at 6 ka BP in summer in the Arctic are models with a relatively low ice extent for present-day conditions (BCC-CSM1-1, CNRM-CM5, HadGEM2-CC, HadGEM2-ES, MRI-CGCM3). Those models are also generally among the ones that show the fastest decrease of the ice extent in the Arctic in projections for the 21st century (Massonnet et al., 2012; Stroeve et al., 2012). However, because the forcings are very different in the two periods and the models response can be dominated by many different feedbacks, the link is not systematic. For instance, the MIROC-ESM, which has the lowest ice extent in the Arctic for present-day condition among the PMIP3 models, simulates a very fast decrease of the ice extent during the 21st century (Massonnet et al., 2012) but has only very moderate changes for 6 ka BP (Berger et al., 2013).

By contrast, if it is expected that models with a large ice extent for modern conditions will also have a large one at LGM, it is not obvious to determine a priori if they will also show a larger increase in this period compared to the other models. At this stage, PMIP2 and PMIP3 results do not bring any clear answer except in winter in the Southern Hemisphere where it appears to be indeed the case (Fig. 4), but this aspect certainly deserves additional attention.

Those results highlight the interest in understanding the causes of the discrepancies between observed and simulated sea ice cover for present-day conditions before analysing past periods. However, as sea ice is strongly coupled to the atmosphere and the ocean, the inability of models to reproduce some of the sea ice characteristics are not necessarily linked to the sea ice model itself but also to its ocean or atmospheric components. Identifying the causes of the biases is therefore a very complex and time demanding task. It is even not always clear to determine exactly why a model version behaves in a different way than the previous one (e.g., Voldoire et al., 2012; Landrum et al., 2012). Nevertheless, the studies that have been devoted to the subject have identified several potential sources of error.

First, for the sea ice model, it seems important to reproduce well the thermodynamics of the system by including a multi-category scheme that takes into account adequately the sub-grid scale distribution of ice thickness and to have a good representation of surface albedo, at least for the Arctic (e.g. Holland et al., 2010; Landrum et al., 2012). Furthermore, many models do not reproduce well the coupling between sea ice thickness and ice dynamics in the Arctic, simulating higher velocities during the months when ice is thick than when it is thin in contrast to observations, with a potential impact on the ice transport, on the regional distribution of the ice and on the response of the model to the forcing (Rampal et al., 2011).

Secondly, some systematic model biases for sea ice have been related to the simulated winds and ocean currents. In CCSM3 and CCSM4, the too strong winds in the Southern Ocean induce a too large northward sea ice transport, contributing to the overestimation of the sea ice extent in those models (Landrum et al., 2012). In a similar way, Koldunov et al. (2010) relate some discrepancies between observed and simulated ice thickness and concentration in ECHAM5/MPI-OM to a spurious atmospheric circulation around the North Pole in this model. Illustrating the role of ocean currents, Voldoire et al. (2012) argue that the simulated sea ice extent is greatly improved in the Barents Sea in the new version of the CNRM model (CNRM-CM5.1) thanks to a better representation of the northward oceanic heat transport and of the currents there. Because of their resolution, no model currently used in the framework of CMIP5 can explicitly represent the meso-scale eddies that plays a dominant role in ocean dynamics, in particular in the Southern Ocean (e.g., Böning et al., 2008). Their effects are thus parameterized in different ways in models with consequences on the simulated mean state of the model and on the response of ocean circulation and oceanic heat transport to changes in wind forcing (e.g., Farneti and Gent, 2011; Gent and Danabosoglu, 2011).

Thirdly, the heat fluxes at the top and the bottom of sea ice are influenced by the way models simulate the structure of the oceanic and atmospheric boundary layers. In the Arctic, many models overestimate the strength of the temperature inversion in winter, with a clear impact on both turbulent and radiative fluxes (Boé et al., 2009b). In the Southern Ocean, the stability of the water column plays a dominant role because it controls the vertical oceanic heat input to the ocean surface and the sea ice. Unfortunately, the majority of the models are not able to adequately reproduce the observed stratification and the processes responsible for the exchange between the surface oceanic layer and the deeper ones, explaining some of the discrepancies between model and data and between different models in this region (e.g., Arzel et al., 2006; Russell et al., 2006; Lefebvre and Goosse, 2008; Sen Gupta et al., 2009). Additionally, the radiative fluxes are influenced by clouds and any bias in their representation has a large effect on surface fluxes in polar regions (e.g., Bodas-Salcedo et al., 2012).

The ability to reproduce well the mean state for present-day conditions is a key indicator of model behaviour but it also necessary to evaluate its response to perturbations. A large part of the work devoted to this subject has been focussed on future change and thus on the impact of an increase in radiative forcing. Unsurprisingly, it has been shown that the decline in sea ice is well correlated with the temperature increase in the Arctic but many models display a too low decrease in sea ice area per degree of warming (e.g. Mahlstein and Knutti, 2012). There is also a large scatter in the simulated polar amplification of the temperature changes (i.e., the ratio between the warming in polar regions and the one at global scale) both for future and past conditions (e.g., Holland and Bitz, 2003; Masson-Delmotte et al., 2006; Mahlstein and Knutti, 2012), leading to very different response at high latitudes between models that display similar global mean temperature changes.

Part of this spread in model results has been related to the different magnitude of standard feedbacks in the various models, in particular the ones associated with clouds, surface albedo, and clear sky longwave fluxes (e.g., Holland and Bitz, 2003; Crucifix, 2006; Qu and Hall, 2006; Boé et al., 2010). In turn, a fraction of the scatter in the magnitude of feedbacks can be linked to the model biases for present-day conditions. For instance, Boé et al. (2009b) argue that the vertical stability of the atmosphere in winter in the Arctic controls the magnitude of the temperature changes which is a dominant contributor in the spread in the longwave feedback. In models with a too strong temperature inversion, the warming caused by the radiative forcing tends to remain confined close to the surface, inducing a larger increase in upward longwave fluxes and thus a larger negative longwave feedback which damps the temperature and sea ice responses.

Atmospheric and oceanic circulations also respond differently in the various models to perturbations, leading to modifications in the heat transport towards high latitudes which can be a significant contributor to the climate changes there (e.g., Holland and Bitz, 2003; Bitz et al., 2006; Mahlstein and Knutti, 2011; Serreze and Barry, 2011) . In this framework, the wide range of the magnitude of the deep circulation in the North Atlantic simulated for LGM conditions (e.g., Otto-Bliesner et al., 2007) has certainly a large impact on the spread of the sea ice edge in winter in this region. In the Southern Ocean, as already noticed for present-day conditions, the stratification of the ocean and the winds appear to play a dominant role in shaping the model response for both past and future changes (e.g. Lefebvre and Goosse, 2008; Sen Gupta et al., 2009; Roche et al., 2012). In particular, Roche et al. (2012) suggest that the inability of models to simulate a larger amplitude of the seasonal cycle of sea ice extent for LGM conditions compared to present-day is due to a too weak stratification simulated by the models at that time.

This non-exhaustive list shows that the model response results from the interplay of many mechanisms. As a consequence, a model that reproduce reasonably well the majority of them would not necessary obtain results in better agreement with observations compared to a model that appears less realistic on single factors but has a better compensation of errors, by chance or because of a better tuning (e.g., Parkinson et al., 2006). This is illustrated by Roche et al. (2012) who explains that HadCM3, which has one of the simplest sea ice model among all the ones involved in PMIP2 was among the best ones in simulating the sea ice extent in the Southern Ocean at the LGM.

6. Conclusions

In the northern hemisphere, models agree broadly with each other and reproduce the main features of the reconstructions for the periods investigated here. The model spread is much larger in the southern hemisphere, as already noticed for pre-industrial and present-day climate. The simulations of past climates also indicate a strong link with the simulations for modern conditions with the same model. In particular, the models with unrealistic conditions for the recent past are also unrealistic for the more distant periods.

When analysing models results in more details, differences on the magnitude of the response as well as in the regional changes are noticed. The comparison with proxies provides then an additional benchmark for the models that display satisfactory results for present-day conditions. A model can indeed be relatively good for the recent past because of a compensation of errors or because some processes that are not well represented in the model do not play a critical role during this period while they are crucial in the

dynamics of some past and future changes. Adequate tests under past conditions could then underline the behaviour in a wider range of conditions, providing additional confidence in the physics of the models that most successfully agree with proxy data. Furthermore, the reliability of a set of models could also be estimated to see if this ensemble as a group represents well the variability deduced from data. To be useful, those tests must correspond to periods where the difference between model results is large enough. In this framework, the mid-Holocene is an interesting candidate, in particular for summer ice extent in the Arctic, but the signal is still relatively small. Besides, the early Holocene and the LGM display more contrasted changes. It is also possible to rank the models in order to select the ones that can be used with the highest confidence to study a specific past period. This should however be done with caution as a good model for some variables or in some regions is not necessary the best for some other ones. Reducing the range of model results by selecting only some of them could then lead to overconfident interpretations that do not cover the full range of uncertainty.

All the models results may differ from some proxy evidence. A first point is then to ensure that the proxy signal is robust and that no alternative and reasonable interpretation of the proxy can reconcile models and data. If this is not possible, this provides a clear target for improving our understanding the dynamics of the system and its modelling. For instance, models fail to represent the sea-ice distribution in the Southern Ocean for the LGM both in shape and in seasonal range, calling for a detailed assessment of mechanisms driving sea-ice changes over such timescales (e.g., Roche et al., 2012). During the early Holocene, many proxies suggest a larger retreat of sea ice north and east of Greenland while sea ice was still likely present in a large fraction of the Canadian Basin of the Arctic. No model is able to reproduce such a feature reasonably well, maybe because it is related to some circulation changes at high latitudes in response to the forcing they are not able to simulate adequately (e.g., de Vernal et al., 2005; Dyck et al., 2010; Funder et al., 2011).

In addition to the general model benchmarking, simulations of past climate and model–data comparison can also focus on some important, specific processes such as the atmospheric and oceanic circulation changes in response to modifications of the surface temperature gradients or the influence of a freshwater discharge at high latitudes. The latter seems particularly interesting since many questions have been raised on the impact an additional freshwater discharge from Greenland in the future. The last deglaciation, or the Eemian provides then a nice way to investigate the relative magnitude of the response to the radiative forcing compared to the ones of the freshwater input in conditions relatively similar to the present ones, both locally as well as in remote areas through teleconnections (e.g., Renssen et al., 2009, 2010; Govin et al., 2012).

In summary, the examples presented here of simulations of past sea ice states have illustrated that having a good quantitative response of the system to a perturbation, the right spatial distribution and a reasonable confidence of the mechanisms involved is important for improving models, models that can in turn improve our understanding of the system. This is also essential for our confidence in projections as several studies have demonstrate the link between past and future changes and the interest of past simulations for evaluating the quality of simulated future changes (e.g., Masson-Delmotte et al., 2006; Goosse et al., 2007; Miller et al., 2010; Schmidt, 2010; Braconnot et al., 2012; Vandenberghe et al., 2012).

Acknowledgements

This paper was written as part of the Sea Ice Proxies working group funded by PAGES (Past Global Changes). We would like to thank all the scientists that made their data and model results available to us, in particular H. Renssen, J Jungclaus and N. Fischer. We acknowledge the World Climate Research Programme's Working Group on Coupled Modelling, which is responsible for CMIP. For CMIP the U.S. Department of Energy's Program for Climate Model Diagnosis and Intercomparison provides coordinating support and led development of software infrastructure in partnership with the Global Organization for Earth System Science Portals. We also thank the Laboratoire des Sciences du Climat et de l'Environnement (LSCE) for collecting and archiving the PMIP model data. The PMIP Data Archive is supported by CEA, CNRS and the Programme National d'Etude de la Dynamique du Climat (PNEDC). H.G. is Senior Research Associate with the Fonds National de la Recherche Scientifique (F.R.S.–FNRS-Belgium). This work is supported by the F.R.S.–FNRS and by the Belgian Federal Science Policy Office (Research Program on Science for a Sustainable Development). The research leading to these results has received funding from the European Union's Seventh Framework programme (FP7/2007-2013) under grant agreement no 243908, "Past4Future. Climate change – Learning from the past climate.". Computational resources have been provided by the supercomputing facilities of the Université catholique de Louvain (CISM/UCL) and the Consortium des Equipements de Calcul Intensif en Fédération Wallonie Bruxelles (CECI) funded by the Fond de la Recherche Scientifique de Belgique (FRS–FNRS). D.M.R acknowledges funding from the CNRS through the LEFE-EVE RISCC project, NWO through the VI-scheme, AC^{2}ME VIDI research grant n°864.09.013 and through the EU (project Past4Future). This is Past4Future contribution 43.

References

Annan, J.D., Hargreaves, J.C., 2006. Using multiple observationally based constraints to estimate climate sensitivity. Geophysical Research Letters 33 (L06704). http://dx.doi.org/10.1029/2005GL025259.

Arzel, O., Fichefet, T., Goosse, H., 2006. Sea ice evolution over the 20th and 21st centuries as simulated by current AOGCM. Ocean Modelling 12, 401–415.

Berger, A., 1978. Long-term variations of daily insolation and Quaternary climatic changes. Journal of Atmospheric Sciences 35, 2363–2367.

Berger, A., Loutre, M.F., 1991. Insolation values for the last 1000000 years. Quaternary Science Reviews 10, 297–317.

Berger, M., Brandefelt, J., Nilsson, J., 2013. The sensitivity of the Arctic sea ice to orbitally-induced insolation changes; a study of the mid-Holocene Paleoclimate Modelling Intercomparison Project 2 and 3 simulations. Climate of the Past. in press.

Bitz, C.M., Roe, G.H., 2004. A mechanism for the high rate of sea ice thinning in the Arctic Ocean. Journal of Climate 17 (18), 3623–3632.

Bitz, C.M., Gent, P.R., Woodgate, R.A., Holland, M.M., Lindsay, R., 2006. The influence of sea ice on ocean heat uptake in response to increasing CO_2. Journal of Climate 19, 2437–2450.

Bodas-Salcedo, A., Williams, K.D., Field, P.R., Lock, A.P., 2012. The surface downwelling solar radiation surplus over the Southern Ocean in the Met Office Model: the role of midlatitude cyclone clouds. Journal of Climate 25, 4817–4838.

Boé, J., Hall, A., Qu, X., 2009a. September sea-ice cover in the Arctic Ocean projected to vanish by 2100. Nature Geoscience 2, 341–343.

Boé, J., Hall, A., Qu, X., 2009b. Current GCMs' unrealistic negative feedback in the Arctic. Journal of Climate 22, 4682–4695.

Boé, J., Hall, A., Qu, X., 2010. Sources of spread in simulations of Arctic sea ice loss over the twenty-first century. Climatic Change 99, 637–645.

Böning, C.W., Dispert, A., Visbeck, M., Rintoul, S.R., Schwarzkopf, F.U., 2008. The response of the Antarctic Circumpolar Current to recent climate change. Nature Geoscience 1, 864–869.

Braconnot, P., Otto-Bliesner, B., Harrison, S., Joussaume, S., Peterchmitt, J.Y., Abe-Ouchi, A., Crucifix, M., Driesschaert, E., Fichefet, T., Hewitt, C.D., Kageyama, M., Kitoh, A., Lan, A., Loutre, M.F., Marti, O., Merkel, U., Ramstein, G., Valdes, P., Weber, S.L., Yu, Y., Zhao, Y., 2007a. Results of PMIP2 coupled simulations of the Mid-Holocene and Last Glacial Maximum – part 1: experiments and large-scale features. Climate of the Past 3, 261–277.

Braconnot, P., Otto-Bliesner, B., Harrison, S., Joussaume, S., Peterchmitt, J.-Y., Abe-Ouchi, A., Crucifix, M., Driesschaert, E., Fichefet, T., Hewitt, C.D., Kageyama, M., Kitoh, A., Loutre, M.-F., Marti, O., Merkel, U., Ramstein, G., Valdes, P., Weber, S.L., Yu, Y., Zhao, Y., 2007b. Results of PMIP2 coupled simulations of the Mid-Holocene and Last Glacial Maximum part 2: feedbacks with emphasis on the location of the ITCZ and mid- and high latitudes heat budget. Climate of the Past 3, 279–296.

Braconnot, P., Harrison, S.P., Kageyama, M., Bartlein, P.J., Masson-Delmotte, V., Abe-Ouchi, A., Otto-Bliesner, B., Zhao, Y., 2012. Evaluation of climate models using palaeoclimatic data (Review). Nature Climate Change 2, 417–424.
Calov, R., Ganopolski, A., Claussen, M., Petoukhov, V., Greve, R., 2005. Transient simulation of the Last Glacial inception. Part I: glacial inception as a bifurcation in the climate system. Climate Dynamics 24, 545–561.
Cavalieri, D.J., Parkinson, C.L., 2012. Arctic sea ice variability and trends, 1979–2010. The Cryosphere 6, 881–889.
Comiso, J.C., Nishio, F., 2008. Trends in the sea ice cover using enhanced and compatible AMSR-E, SSM/I, and SMMR data. Journal of Geophysical Research 113 (C02S07). http://dx.doi.org/10.1029/2007JC004257.
Crespin, E., Goosse, H., Fichefet, T., Mairesse, A., Sallaz-Damaz, Y., 2013. Arctic climate over the past millennium: annual and seasonal responses to external forcings. The Holocene 23 (3), 319–327.
Crucifix, M., Loutre, M.F., 2002. Transient simulations over the Last Interglacial period (126–115 kyr BP): feedback and forcing analysis. Climate Dynamics 19, 417–433.
Crucifix, M., 2006. Does the Last Glacial Maximum constrain climate sensitivity? Geophysical Research Letters 33 (18), L18701.
de Vernal, A., Hillaire-Marcel, C., Turon, J.-L., Matthiessen, J., 2000. Reconstruction of sea-surface temperature, salinity, and sea-ice cover in the northern North Atlantic during the Last Glacial Maximum based on dinocyst assemblages. Canadian Journal of Earth Sciences 37, 725–750.
de Vernal, A., Hilaire-Marcel, C., Darby, D.A., 2005. Variability of the ice cover in the Chukchi Sea (western Arctic Ocean) during the Holocene. Paleoceanography 20 (PA4018). http://dx.doi.org/10.1029/2005PA001157.
Dyck, S., Tremblay, L.B., de Vernal, A., 2010. Arctic sea-ice cover from the early Holocene: the role of atmospheric circulation patterns? Quaternary Science Reviews 29, 3457–3467.
Ebert, E.E., Curry, J.A., 1993. An intermediate one-dimensional thermodynamic sea ice model for investigating ice-atmosphere interactions. Journal of Geophysical Research 98 (C6), 10085–10109.
Edwards, T., Crucifix, M., Harrison, S., 2007. Using the past to constrain the future: how the palaeorecord can improve estimates of global warming. Progress in Physical Geography 31, 481–500.
Farneti, R., Gent, P.R., 2011. The effects of the eddy-induced advection coefficient in a coarse-resolution coupled climate model. Ocean Modelling 39, 135–145.
Fetterer, F., Knowles, K., Meier, W., Savoie, M., 2012. Sea Ice Index. Electronic. Available at: http://nsidc.org/data/seaice index/ (last accessed July 2012).
Fischer, N., Jungclaus, J.H., 2011. Evolution of the seasonal temperature cycle in a transient Holocene simulation: orbital forcing and sea-ice. Climate of the Past 7, 1139–1148.
Flanner, M.G., Shell, K.M., Barlage, M., Perovich, D.K., Tschudi, M.A., 2011. Radiative forcing and albedo feedback from the Northern Hemisphere cryosphere between 1979 and 2008. Nature Geoscience 4, 151–155.
Flocco, D., Feltham, D.L., Turner, A.K., 2010. Incorporation of a physically based melt pond scheme into the sea ice component of a climate model. Journal of Geophysical Research 115 (C08012). http://dx.doi.org/10.1029/2009JC005568.
Fukamachi, Y., Ohshila, K.I., Mukai, Y., Mizuta, G., Wakatsuchi, M., 2011. Sea-ice drift characteristics revealed by measurements of acoustic Doppler current profiler and ice-profiling sonar off Hokkaido in the Sea of Okhotsk. Annals of Glaciology 52, 1–8.
Funder, S., Goosse, H., Jepsen, H., Kaas, E., Kjær, K.H., Korsgaard, N.J., Larsen, N.K., Linderson, H., Lyså, A., Möller, P., Olsen, J., Willerslev, E., 2011. A 10,000 yr record of Arctic Ocean sea ice variability – view from the beach. Science 333, 747–750.
Gent, P.R., Danabosoglu, G., 2011. Response to increasing Southern Hemisphere winds in CCSM4. Journal of Climate 24, 4992–4998.
Gent, P.R., Danabasoglu, G., Donner, L.J., Holland, M.M., Hunke, E.C., Jayne, S.R., Lawrence, D.M., Neale, R.B., Rasch, P.J., Vertenstein, M., Worley, P.H., Yang, Z.-L., Zhang, M., 2011. The community climate system model version 4. Journal of Climate 24, 4973–4991.
Gersonde, R., Crosta, X., Abelmann, A., Armand, L., 2005. Sea-surface temperature and sea ice distribution of the Southern Ocean at the EPI LOG Last Glacial Maximum: a circum-Antarctic view based on siliceous microfossil records. Quaternary Science Reviews 24, 869–896.
Gloersen, P., Parkinson, C.L., Cavalieri, D.J., Comiso, J.C., Zwally, H.J., 1999. Spatial distribution of trends and seasonality in the hemispheric sea ice covers: 1978–1996. Journal of Geophysical Research 104 (C9), 20,827–20,835.
Gordon, C., Cooper, C., Senior, C.A., Banks, H., Gregory, J.M., Johns, T.C., Mitchell, J.F.B., Wood, R.A., 2000. The simulation of SST, sea ice extents and ocean heat transports in a version of the Hadley Centre coupled model without flux adjustments. Climate Dynamics 16, 147–168.
Goosse, H., Driesschaert, E., Fichefet, T., Loutre, M.-F., 2007. Information on the early Holocene climate constrains the summer sea ice projections for the 21st century. Climate of the Past 3, 683–692.
Goosse, H., Arzel, O., Bitz, C.M., de Montety, A., Vancoppenolle, M., 2009. Increased variability of the Arctic summer ice extent in a warmer climate. Geophysical Research Letters 36, L23702. http://dx.doi.org/10.1029/2009GL040546.
Goosse, H., Brovkin, V., Fichefet, T., Haarsma, R., Jongma, J., Huybrechts, P., Mouchet, A., Selten, F., Barriat, P.-Y., Campin, J.-M., Deleersnijder, E., Driesschaert, E., Goelzer, H., Janssens, I., Loutre, M.-F., Morales Maqueda, M.A., Opsteegh, T., Mathieu, P.-P., Munhoven, G., Petterson, E., Renssen, H., Roche, D.M., Schaeffer, M., Severijns, C., Tartinville, B., Timmermann, A., Weber, N., 2010. Description of the earth system model of intermediate complexity LOVECLIM version 1.2. Geoscientific Model Development 3, 603–633.
Goosse, H., Braida, M., Crosta, X., Mairesse, A., Masson-Delmotte, V., Mathiot, P., Neukom, R., Oeter, H., Philippon, G., Renssen, H., Stenni, B., van Ommen, T., Verleyen, E., 2012. Antarctic temperature changes during the last millennium: evaluation of simulations and reconstructions. Quaternary Science Reviews 55, 75–90.
Govin, A., Braconnot, P., Capron, E., Cortijo, E., Duplessy, J.-C., Jansen, E., Labeyrie, L., Landais, A., Marti, O., Michel, E., Mosquet, E., Risebrobakken, B., Swingedouw, D., Waelbroeck, C., 2012. Persistent influence of ice sheet melting on high northern latitude climate during the early Last Interglacial. Climate of the Past 8, 483–507.
Hargreaves, J.C., Paul, A., Ohgaito, R., Abe-Ouchi, A., Annan, J.D., 2011. Are paleoclimate model ensembles consistent with the MARGO data synthesis? Climate of the Past 7, 917–933.
Hargreaves, J.C., Annan, J.D., Ohgaito, R., Paul, A., Abe-Ouchi, A., 2012. Skill and reliability of climate model ensembles at the Last Glacial Maximum and mid Holocene. Climate of the Past Discussions 8, 3481–3511.
Hewitt, C., Stouffer, R., Broccoli, A., Mitchell, J., Valdes, P., 2003. The effect of ocean dynamics in a coupled GCM simulation of the Last Glacial Maximum. Climate Dynamics 20, 203–218.
Hibler, W.D., 1979. A dynamic thermodynamic sea ice model. Journal of Physical Oceanography 9, 815–846.
Holland, M.M., Bitz, C.M., 2003. Polar amplification of climate change in coupled models. Climate Dynamics 21, 221–232.
Holland, M., Serreze, M.M., Stroeve, J., 2008. The sea ice mass budget of the Arctic and its future change as simulated by coupled climate models. Climate Dynamics 34, 185–200.
Holland, M.M., Serreze, M.C., Stroeve, J., 2010. The sea ice mass budget of the Arctic and its future change as simulated by coupled climate models. Climate Dynamics 34, 185–200.
Hunke, E.C., Lipscomb, W.H., 2010. CICE: the Los Alamos Sea Ice Model. Documentation and Software User's Manual, Version 4.1, Tech. Rep. LA-CC-06-012. Los Alamos National Laboratory, Los Alamos, New Mexico.
Hunke, E.C., Lipscomb, W.H., Turner, A.K., 2010. Sea-ice models for climate study: retrospective and new directions. Journal of Glaciology 56, 1162–1172.
Jacob, R., Schafer, C., Foster, I., Tobis, M., Andersen, J., 2001. Computational design and performance of the fast ocean atmosphere model: version 1. In: The 2001 International Conference of Computational Science, pp. 175–184, 25.
Johns, T., Gregory, J., Ingram, W., Johnson, C., Jones, A., Lowe, J., Mitchell, J., Roberts, D., Sexton, D., Stevenson, D., Tett, S., Woodag, M., 2003. Anthropogenic climate change for 1860 to 2100 simulated with the HadCM3 model under updated emissions scenarios. Climate Dynamics 20, 583–612.
Jungclaus, J.H., Lorenz, S.J., Timmreck, C., Reick, C.H., Brovkin, V., Six, K., Segschneider, J., Giorgetta, M.A., Crowley, T.J., Pongratz, J., Krivova, N.A., Vieira, L.E., Solanki, S.K., Klocke, D., Botzet, M., Esch, M., Gayler, V., Haak, H., Raddatz, T.J., Roeckner, E., Schnur, R., Widmann, H., Claussen, M., Stevens, B., Marotzke, J., 2010. Climate and carbon-cycle variability over the last millennium. Climate of the Past 6 (5), 723–737.
K-1-Model-Developers, 2004. K-1 Coupled GCM (MIROC Description). Tech. Rep., CCSR/NIES/FRCGC, 25.
Kaufman, D.S., Schneider, D.P., McKay, N.P., Ammann, C.M., Bradley, R.S., Briffa, K.R., Miller, G.H., Otto-Bliesner, B.L., Overpeck, J.T., Vinther, B.M., Arctic Lakes 2k Project Members, 2009. Recent warming reverses long-term Arctic cooling. Science 325, 1236–1239.
Kay, J.E., Gettelman, A., 2009. Cloud influence on and response to seasonal Arctic sea ice loss. Journal of Geophysical Research 114, D18204. http://dx.doi.org/10.1029/2009JD011773.
Kay, J.E., Raeder, J.E., Gettelman, A., Anderson, J., 2011. The boundary layer response to recent Arctic sea ice loss and implications for high-latitude climate feedbacks. Journal of Climate 24, 428–447.
Kinnard, C., Zdanowicz, C.M., Fisher, D.A., Isaksson, E., de Vernal, A., Thompson, L.G., 2011. Reconstructed changes in Arctic sea ice over the past 1450 years. Nature 479, 509–512.
Koldunov, N.V., Stammer, D., Marotzke, J., 2010. Present-day Arctic sea ice variability in the coupled ECHAM5/MPI-OM model. Journal of Climate 23, 2520–2543.
Kucera, M., Weinelt, M., Kiefer, T., Pflaumann, U., Hayes, A., Weinelt, M., Chen, M.T., Mix, A.C., Barrows, T.T., Cortijo, E., Duprat, J., Juggins, S., Waelbroeck, C., 2005. Reconstruction of sea-surface temperatures from assemblages of planktonic foraminifera: multi-technique approach based on geographically constrained calibration datasets and its application to glacial Atlantic and Pacific Oceans. Quaternary Science Reviews 24, 951–998.
Landrum, L., Holland, M.M., Schneider, D.P., Hunke, E., 2012. Antarctic sea ice climatology, variability, and late twentieth-century change in CCSM4. Journal of Climate 25, 4817–4838.
Lecomte, O., Fichefet, T., Vancoppenolle, M., Nicolaus, M., 2011. A new snow thermodynamic scheme for large scale sea-ice models. Annals of Glaciology 52, 337–346.
Lefebvre, W., Goosse, H., 2008. Analysis of the projected regional sea-ice changes in the Southern Ocean during the 21st century. Climate Dynamics 30, 59–76.
Lohmann, G., Pfeiffer, M., Laepple, T., Leduc, G., Kim, J.-H., 2012. A model-data comparison of the Holocene global sea surface temperature evolution. Climate of the Past Discussions 8, 1005–1056.
Mahlstein, I., Knutti, R., 2011. Ocean heat transport as a cause for model uncertainty in projected arctic warming. Journal of Climate 24, 1451–1460.

Mahlstein, I., Knutti, R., 2012. September Arctic sea ice predicted to disappear near 2°C global warming above present. Journal of Geophysical Research 117 (D06104). http://dx.doi.org/10.1029/2011JD016709.
Marsland, S.J., Haak, H., Jungclaus, J.H., Latif, M., Röske, F., 2003. The Max-Planck-Institute global ocean/sea ice model with orthogonal curvilinear coordinates. Ocean Modelling 5, 91–127.
Marti, O., Braconnot, P., Bellier, J., Benshila, R., Bony, S., Brockmann, P., Cadule, P., Caubel, A., Denvil, S., Dufresne, J.L., Fairhead, L., Filiberti, M.A., Foujols, M.A., Fichefet, T., Friedlingstein, P., Goosse, H., Grandpeix, J.Y., Hourdin, F., Krinner, G., Lévy, C., Madec, G., Musat, I., de Noblet, N., Polcher, J., Talandier, C., 2005. The New IPSL Climate System Model: IPSL-CM4. In: Notes du Pôle de Modélisation 26. Institut Pierre Simon Laplace des Sciences de l'Environnement Global, Case 101, 4 place Jussieu, 75252 Paris Cedex5, France.
Martin, G.M., Bellouin, N., Collins, W.J., Culverwell, I.D., Halloran, P.R., Hardiman, S.C., Hinton, T.J., Jones, C.D., McDonald, R.E., McLaren, A.J., O'Connor, F.M., Roberts, M.J., Rodriguez, J.M., Woodward, S., Best, M.J., Brooks, M.E., Brown, A.R., Butchart, N., Dearden, C., Derbyshire, S.H., Dharssi, I., Doutriaux-Boucher, M., Edwards, J.M., Falloon, P.D., Gedney, N., Gray, L.J., Hewitt, H.T., Hobson, M., Huddleston, M.R., Hughes, J., Ineson, S., Ingram, W.J., James, P.M., Johns, T.C., Johnson, C.E., Jones, A., Jones, C.P., Joshi, M.M., Keen, A.B., Liddicoat, S., Lock, A.P., Maidens, A.V., Manners, J.C., Milton, S.F., Rae, J.G.L., Ridley, J.K., Sellar, A., Senior, C.A., Totterdell, I.J., Verhoef, A., Vidale, P.L., Wiltshire, A., 2011. The HadGEM2 family of Met Office Unified Model climate configurations. Geoscientific Model Development 4, 723–757.
Martinson, D.G., 1990. Evolution of the Southern Ocean winter mixed layer and sea ice: open ocean deepwater formation and ventilation. Journal of Geophysical Research 95, 11641–11654.
Martinson, D.G., Steele, M., 2001. Future of the Arctic Sea ice cover' implications of an antarctic analog. Geophysical Research Letters 28, 307–310.
Masson-Delmotte, V., Kageyama, M., Braconnot, P., Charbit, S., Krinner, G., Ritz, C., Guilyardi, E., Jouzel, J., Abe-Ouchi, A., Crucifix, M., Gladstone, R., Hewitt, C., Kitoh, A., LeGrande, A., Marti, O., Merkel, U., Motoi, T., Ohgaito, R., Otto-Bliesner, B., Peltier, W., Ross, I., Valdes, P., Vettoretti, G., Weber, S., Wolk, F., Yu, Y., 2006. Past and future polar amplification of climate change: climate model intercomparisons and ice-core constraints. Climate Dynamics 26, 513–529.
Massonnet, F., Fichefet, T., Goosse, H., Vancoppenolle, M., Mathiot, P., König Beatty, C., 2011. On the importance of physics in hindcast simulations of Arctic and Antarctic Sea ice. The Cryosphere 5, 687–699.
Massonnet, F., Fichefet, T., Goosse, H., Bitz, C.M., Philippon-Berthier, G., Holland, M.M., Barriat, P.-Y., 2012. The mean sea ice state as a reasonable criterion to constrain projections of summer Arctic sea ice. The Cryosphere 6, 1383–1394.
Maykut, G.A., Untersteiner, N., 1971. Some results from a time-dependent thermodynamic model of sea ice. Journal of Geophysical Research 76 (6), 1550–1575.
Maykut, G.A., 1982. Large-scale heat exchange and ice production in the Central Arctic. Journal of Geophysical Research 87 (C10), 7971–7984.
Miller, G.H., Alley, R.B., Brigham-Grette, J., Fitzpatrick, J.J., Polyak, L., Serreze, M.C., White, J.W.C., 2010. Arctic amplification: can the past constrain the future? Quaternary Science Reviews 29, 1779–1790.
Miller, G.H., Geirsdóttir, A., Zhong, Y., Larsen, D.J., Otto-Bliesner, B.L., Holland, M.M., Bailey, D.A., Refsnider, K.A., Lehman, S.J., Southon, J.R., Anderson, C., Björnsson, H., Thordarson, T., 2012. Abrupt onset of the Little Ice Age triggered by volcanism and sustained by sea-ice/ocean feedbacks. Geophysical Research Letters 39, L02708. http://dx.doi.org/10.1029/2011GL050168.
Otto-Bliesner, B.L., Brady, E.C., Clauzet, G., Tomas, R., Levis, S., Kothavala, Z., 2006. Last Glacial Maximum and Holocene climate in CCSM3. Journal of Climate 19, 2526–2544.
Otto-Bliesner, B.L., Hewitt, C.D., Marchitto, T.M., Brady, E., Abe-Ouchi, A., Crucifix, M., Murakami, S., Weber, S.L., 2007. Last Glacial Maximum ocean thermohaline circulation: PMIP2 model intercomparisons and data constraints. Geophysical Research Letters 34 (L12706). http://dx.doi.org/10.1029/2007GL029475.
Parkinson, C.L., Washington, W.M., 1979. A large-scale numerical model of sea ice. Journal of Geophysical Research 84 (C1), 311–336.
Parkinson, C.L., Cavalieri, D.J., Gloersen, P., Zwally, H.J., Comiso, J.C., 1999. Arctic sea ice extents, areas and trends, 1978–1996. Journal of Geophysical Research 97, 17,715–17,728.
Parkinson, C.L., Vinnikov, K.Y., Cavalieri, D.J., 2006. Evaluation of the simulation of the annual cycle of Arctic and Antarctic sea ice coverages by 11 major global climate models. Journal of Geophysical Research 111 (C7), C07012.
Parkinson, C.L., Cavalieri, D.J., 2012. Antarctic sea ice variability and trends, 1979–2010. The Cryosphere 6, 871–880.
Peltier, W., 2004. Global glacial isostasy and the surface of the Ice-Age Earth: the ICE-5G (VM2) model and GRACE. Annual Review of Earth and Planetary Sciences 32, 111–149.
Perovich, D.K., Light, B., Eicken, H., Jones, K.F., Runciman, K., Nghiem, S.V., 2007. Increasing solar heating of the Arctic Ocean and adjacent seas, 1979–2005: attribution and role in the ice-albedo feedback. Geophysical Research Letters 34, L19505. http://dx.doi.org/10.1029/2007GL031480.
Perovich, D.K., Richter-Menge, J.A., Jones, K.F., Light, B., 2008. Sunlight, water, and ice: extreme Arctic sea ice melt during the summer of 2007. Geophysical Research Letters 35 (L11501). http://dx.doi.org/10.1029/2008GL034007.
Pflaumann, U., Sarnthein, M., Chapman, M., d'Abreu, L., Funnell, B., Huels, M., Kiefer, T., Maslin, M., Schulz, H., Swallow, J., van Kreveld, S., Vautravers, M., Vogelsang, E., Weinelt, M., 2003. Glacial North Atlantic: sea-surface conditions reconstructed by GLAMAP 2000. Paleoceanography 18 (3), 1065. http://dx.doi.org/10.1029/2002PA000774.
Phipps, S.J., 2006. The CSIRO Mk3L Climate System Model. Tech. Rep.. Antarctic Climate and Ecosystems CRC, University of Tasmania, Institute of Antarctic and Southern Ocean Studies, p. 25.
Phipps, S.J., Rotstayn, L.D., Gordon, H.B., Roberts, J.L., Hirst, A.C., Budd, W.F., 2011. The CSIRO Mk3L climate system model version 1.0-part 1: description and evaluation. Geoscientific Model Development 4, 483–509.
Qu, X., Hall, A., 2006. Assessing snow albedo feedback in simulated climate change. Journal of Climate 19, 2617–2630.
Raddatz, T.J., Reick, C.H., Knorr, W., Kattge, J., Roeckner, E., Schnur, R., Schnitzler, K.-G., Wetzel, P., Jungclaus, J., 2007. Will the tropical land biosphere dominate the climate-carbon cycle feedback during the twenty first century? Climate Dynamics 29, 565–574.
Rampal, P., Weiss, J., Dubois, C., Campin, J.-M., 2011. IPCC climate models do not capture Arctic sea ice drift acceleration: consequences in terms of projected sea ice thinning and decline. Journal of Geophysical Research 116 (C00D07). http://dx.doi.org/10.1029/2011JC007110.
Renssen, H., Goosse, H., Fichefet, T., Brovkin, V., Driesschaert, E., Wolk, F., 2005a. Simulating the Holocene climate evolution at northern high latitudes using a coupled atmosphere-sea ice-ocean-vegetation model. Climate Dynamics 24, 23–43.
Renssen, H., Goosse, H., Fichefet, T., Masson-Delmotte, V., Koç, N., 2005b. The Holocene climate evolution in the high-latitude Southern Hemisphere simulated by a coupled atmosphere-sea ice-ocean-vegetation model. The Holocene 15 (7), 951–964.
Renssen, H., Seppä, H., Heiri, O., Roche, D.M., Goosse, H., Fichefet, T., 2009. The influence of the last deglaciation on the spatio-temporal complexity of the Holocene thermal maximum. Nature Geoscience 2, 411–414.
Renssen, H., Goosse, H., Crosta, X., Roche, D.M., 2010. Early Holocene Laurentide Ice Sheet deglaciation causes cooling in the high-latitude Southern Hemisphere through oceanic teleconnection. Paleoceanography 25 (PA3204). http://dx.doi.org/10.1029/2009PA001854.
Renssen, H., Seppä, H., Crosta, X., Goosse, H., Roche, D.M., 2012. Global characterization of the Holocene Thermal Maximum. Quaternary Science Reviews 48, 7–19.
Roche, D., Paillard, D., Cortijo, E., 2004. Constraints on the duration and freshwater release of Heinrich event 4 through isotope modelling. Nature 432, 379–382.
Roche, D.M., Dokken, T.M., Goosse, H., Renssen, H., Weber, S.L., 2007. Climate of the Last Glacial Maximum: sensitivity studies and model-data comparison with the LOVECLIM coupled model. Climate of the Past 3, 205–224, 454.
Roche, D.M., Crosta, X., Renssen, H., 2012. Evaluating Southern Ocean response for the Last Glacial Maximum and pre-industrial climates: PMIP-2 models and data evidence. Quaternary Science Reviews 56, 99–106.
Rotstayn, L.D., Jeffrey, S.J., Collier, M.A., Dravitzki, S.M., Hirst, A.C., Syktus, J.I., Wong, K.K., 2012. Aerosol- and greenhouse gas-induced changes in summer rainfall and circulation in the Australasian region: a study using single-forcing climate simulations. Atmospheric Chemistry and Physics 12, 6377–6404.
Russell, J.L., Stouffer, R.J., Dixon, K.W., 2006. Intercomparison of the Southern Ocean circulation in IPCC coupled model control simulations. Journal of Climate 19, 4560–4575.
Salas-Mélia, D., Chauvin, F., Déqué, M., Douville, H., Gueremy, J., Marquet, P., Planton, S., Royer, J., Tyteca, S., 2005. Description and Validation of the CNRM-CM3 Global Coupled Model. CNRM Technical Re-port 103 [Available from CNRM/GMGEC]. CNRM Technical Report 103. CNRM/GMGEC.
Schneider von Deimling, T., Held, H., Ganopolski, A., Rahmstorf, S., 2006. Climate sensitivity estimated from ensemble simulations of glacial climate. Climate Dynamics 27, 149–163.
Schmidt, G.A., Ruedy, R., Hansen, J.E., Aleinov, I., Bell, N., Bauer, M., Bauer, S., Cairns, B., Canuto, V., Cheng, Y., Del Genio, A., Faluvegi, G., Friend, A.D., Hall, T.M., Hu, Y., Kelley, M., Kiang, N.Y., Koch, D., Lacis, A.A., Lerner, J., Lo, K.K., Miller, R.L., Nazaewnko, L., Oinas, V., Perlwitz, J., Perlwitz, J., Rind, D., Romanou, A., Russell, G.L., Sato, M., Shindell, D.T., Stone, P.H., Sun, S., Tausnev, N., Thresher, D., Yao, M.-S., 2006. Present-day atmospheric simulations using GISS ModelE: comparison to in situ, satellite and reanalysis data. Journal of Climate 19, 153–192, 25.
Schmidt, G.A., LeGrande, A.N., Hoffmann, G., 2007. Water isotope expression of intrinsic and forced variability in a Coupled ocean-atmosphere model. Journal of Geophysical Research 112 (D10103). http://dx.doi.org/10.1029/2006JD007781.
Schmidt, G.A., 2010. Enhancing the relevance of palaeoclimate model/data comparisons for assessments of future climate change. Journal of Quaternary Science 25, 79–87.
Schmidt, G.A., Jungclaus, J.H., Ammann, C.M., Bard, E., Braconnot, P., Crowley, T.J., Delaygue, G., Joos, F., Krivova, N.A., Muscheler, R., Otto-Bliesner, B.L., Pongratz, J., Shindell, D.T., Solanki, S.K., Steinhilber, F., Vieira, L.E.A., 2011. Climate forcing reconstructions for use in PMIP simulations of the last millennium (v1.0). Geoscientific Model Development 4, 33–45.
Sen Gupta, A., Santoso, A., Taschetto, A.S., Ummenhofer, C.C., Trevena, J., England, M.H., 2009. Projected changes to the Southern Hemisphere ocean and sea ice in the IPCC AR4 climate models. Journal of Climate 22 (11), 3047–3078.
Semtner, A.J., 1976. A model for the thermodynamic growth of sea ice in numerical investigations of climate. Journal of Physical Oceanography 6, 379–389.

Serreze, M.C., Barry, R.G., 2011. Processes and impacts of Arctic amplification: a research synthesis. Global and Planetary Change 77, 85–96.
Sime, L.C., Tindall, J.C., Wolff, E.W., Connolley, W.M., Valdes, P.J., 2008. Antarctic isotopic thermometer during a CO_2 forced warming event. Journal of Geophysical Research 113 (D24119). http://dx.doi.org/10.1029/2008JD010395.
Smith, R., Gregory, J., 2012. The Last Glacial cycle: transient simulations with an AOGCM. Climate Dynamics 38, 1545–1559.
Stroeve, J., Holland, M.M., Meier, W., Scambos, T., Serreze, M., 2007. Arctic sea ice decline: faster than forecast. Geophysical Research Letters 34 (L09501). http://dx.doi.org/10.1029/2007GL029703.
Stroeve, J.C., Serreze, M.C., Holland, M.M., Kay, J.E., Malanik, J., Barrett, A.P., 2012. The Arctic's rapidly shrinking sea ice cover: a research synthesis. Climatic Change 110, 1005–1027.
Stocker, T.F., 2002. North-south connections. Science 297, 1814–1815.
Stouffer, R.J., Yin, J., Gregory, J.M., Dixon, K.W., Spelman, M.J., Hurlin, W., Weaver, A.J., Eby, M., Flato, G.M., Hasumi, H., Hu, A., Jungclaus, J.H., Kamenkovich, I.V., Levermann, A., Montoya, M., Murakami, S., Nawrath, S., Oka, A., Peltier, W.R., Robitaille, D.Y., Sokolov, A., Vettoretti, G., Weber, S.L., 2005. Investigating the causes of the response of the thermohaline circulation to past and future climate changes. Journal of Climate 19, 1365–1387.
Timmermann, A., Timm, O., Stott, L., Menviel, L., 2009. The roles of CO_2 and orbital forcing in driving Southern Hemispheric temperature variations during the last 21 000 yr. Journal of Climate 22, 1626–1640.
Thorndike, A.S., Colony, R., 1982. Sea ice motion in response to geostrophic winds. Journal of Geophysical Research 87 (C8), 5845–5852.
Vancoppenolle, M., Fichefet, T., Goosse, H., Bouillon, S., Madec, G., Morales Maqueda, M.A., 2009. Simulating the mass balance and salinity of Arctic and Antarctic sea ice. 1. Model description and validation. Ocean Modelling 27, 33–53.
Vandenberghe, J., Renssen, H., Roche, D., Goosse, H., Velichko, A.A., Gorbunov, A., 2012. Eurasian permafrost instability constrained by reduced sea-ice cover. Quaternary Science Reviews 34, 16–23.
Voldoire, A., Sanchez-Gomez, E., Salas y Mélia, D., Decharme, B., Cassou, C., Sénési, S., Valcke, S., Beau, I., Alias, A., Chevallier, M., Déqué, M., Deshayes, J., Douville, H., Fernandez, E., Madec, G., Maisonnave, E., Moine, M.-P., Planton, S., Saint-Martin, D., Szopa, S., Tyteca, S., Alkama, R., Belamari, S., Braun, A., Coquart, L., Chauvin, F., 2012. The CNRM-CM5.1 global climate model. Climate Dynamics. http://dx.doi.org/10.1007/s00382-011-1259-y.
Wang, M., Overland, J.E., 2012. Summer arctic sea ice will be gone sooner or later – an update from CMIP5 models. Geophysical Research Letters 39, L18501. http://dx.doi.org/10.1029/2012GL052868.
Watanabe, S., Hajima, T., Sudo, K., Nagashima, T., Takemura, T., Okajima, H., Nozawa, T., Kawase, H., Abe, M., Yokohata, T., Ise, T., Sato, H., Kato, E., Takata, K., Emori, S., Kawamiya, M., 2011. MIROC-ESM 2010: model description and basic results of CMIP5-20c3m experiments. Geoscientific Model Development 4, 845–872.
Widmann, M., Goosse, H., van der Schrier, G., Schnur, R., Barkmeijer, J., 2010. Using data assimilation to study extratropical Northern Hemisphere climate over the last millennium. Climate of the Past 6, 627–644.
Yu, Y.Q., Zhang, X.H., Guo, Y.F., 2004. Global coupled ocean-atmosphere general circulation models in Lasg/Iap. Advances in Atmospheric Sciences 21, 444–455, 25.
Yukimoto, S., Noda, A., Kito, A., Hosaka, M., Yoshimura, H., Uchiyama, T., Shibata, K., Arakawa, O., Kusunoki, S., 2006. Present-day climate and climate sensitivity in the Meteorological Research Institute Coupled GCM Version 2.3 (MRI-CGCM2.3). Journal of the Meteorological Society of Japan 84, 333–363.
Zhang, X., Walsh, J.E., 2006. Toward a seasonally ice-covered Arctic Ocean: scenarios from the IPCC AR4 model simulations. Journal of Climate 19, 1730–1747.
Zhang, Q., Sundqvist, H.S., Moberg, A., Körnich, H., Nilsson, J., Holmgren, K., 2010. Climate change between the mid and late Holocene in northern high latitudes – part 2: model-data comparison. Climate of the Past 6, 609–626.
Zhong, Y., Miller, G.H., Otto-Bliesner, B.L., Holland, M.M., Bailey, D.A., Schneider, D.P., Geirsdóttir, Á., 2011. Centennial-scale climate change from decadally-paced explosive volcanism: a coupled sea ice-ocean mechanism. Climate Dynamics 37, 2373–2387.
Zunz, V., Goosse, H., Massonnet, F., 2013. How does internal variability influence the ability of CMIP5 models to reproduce the recent trend in Southern Ocean sea ice extent? The Cryosphere 7, 451–468.